RETERM – Thermal Engineering Vol. 24 (2025) No. 1

CLIMATE CHANGE IMPACT ON PHOTOVOLTAIC PRODUCTION FROM THE PERSPECTIVE OF CLIMATE MODELS: A SYSTEMATIC REVIEW

Araújo, N. M. F. T. S.[a,*], Santos, P. R. A., Abrahão, R.

Climate group, Federal University of Paraíba, Avenue Presid. Castelo Branco, s/n, Campus I, Cidade Universitária, CEP 58051-970, João Pessoa, Paraíba, Brazil. [a] nicolas.araujo@ufersa.edu.br

ARTICLE INFO

Keywords: *solar energy, performance rate, GCM, RCM, forecasting.*

Received: Feb 07, 2025
Reviewed: Feb 17, 2025
Accepted: Mar 03, 2025

ABSTRACT

Higher concentrations of greenhouse gases resulting from anthropogenic actions associated with energy production are one of the causes of climate change. In this context, several efforts have been undertaken in the search for more sustainable alternatives, with photovoltaic (PV) technology standing out among the different possibilities. However, PV production is dependent on future climate variability, which is a source of uncertainty that can hinder energy planning and impair the effectiveness of systems. This study investigates how the authors approached the theme the climate change impacts on photovoltaic production (P_{pv}) from the perspective of simulations using climate models. To this end, a search was carried out using keywords related to the theme at the Web of Science database and, after filtering, it generated a sample of 58 articles on the theme of climate change impact on PV production, which were subjected to a systematic review. With the analysis and classification of the papers, 14 articles were quantified as indirect approach using simulations from climate models. The main GCMs (global climate models) and RCMs (regional climate models) used in each study, as well as the equations for estimating P_{pv} and the meteorological forecast databases, were identified. The studies found in the literature have mainly focused on Africa, Europe and China.

NOMENCLATURE

AOGCM	Atmosphere-ocean GCM
CIT	Cloud image techniques
CSP	Concentrated solar power
CVC	Climate variability and change
GCM	Global climate model
GHG	Greenhouse gases
GMT	Global mean temperature
GWL	Global warming level
HSI	High-speed improvement
IV	Internal variability
LSI	Low-speed improvement
MLT	Machine learning techniques
OTH	Others
PGW	Pseudo-global warming technique
PI	Pre-industrial level
PT	Physical technique
PV	Photovoltaic
P_{pv}	Photovoltaic production
RCM	Regional climate model
RE	Review articles
SA	Statistical Approaches
SCA	Stepwise cluster analysis
ST	Standard reference
TI	Title
TS	Topic
WOS	Web of Science
WRF	Weather Research and Forecasting

1. INTRODUCTION

Climate change is a natural occurrence that has been observed throughout Earth's history [1]. However, the Intergovernmental Panel on Climate Change [2] states that the current increase in average global temperatures is primarily attributed to elevated levels of greenhouse gases (GHGs) in the atmosphere. These higher concentrations of GHGs are a result of human activities, including the burning of fossil fuels and the rapid expansion of urban areas [3]. Associated with energy production services,

* Corresponding author: Araújo, N. M. F. T. S. Climate group, Federal University of Paraíba, Avenue Presid. Castelo Branco, s/n, Campus I, Cidade Universitária, CEP 58051-970, João Pessoa, Paraíba, Brazil. nicolas.araujo@ufersa.edu.br

anthropogenic emissions of GHG and aerosols are one of the historical [4] and future [5] causes of climate change. Recently, discussions on the causes and effects of this phenomenon, associated with the theme of problems in energy demand and consumption, have increased and gained attention in various debates around the world. There are different options to reduce GHG emissions and simultaneously meet the human demand for energy services that is expected to increase due to climate change [6, 7].

Given this scenario, renewable energy fills the gap between climate and energy sciences, playing a very important role in strategies for decarbonization and mitigation of the adverse effects of climate change [8] and its possible consequences on societies and on the environment [2]. The report of the Intergovernmental Panel on Climate Change [4] suggested that notable alterations in future climate projections will lead to substantial governmental investments in energy and drive innovation in the energy sector [9]. In efforts to accomplish the objective of carbon emissions reduction, there has been a significant global increase in the deployment of renewable energy sources [10].

Photovoltaic (PV) energy generation, which involves the direct conversion of sunlight into electricity, has shown significant growth potential and has the ability to eventually rival conventional energy sources [11]. The decline in the cost of PV systems and advancements in energy production efficiency [12] have played a key role in the increased installation of PV panels. There are other factors that contribute to the popularity of PV technology: easy implementation, modularity, low maintenance and, mainly, a fast-learning curve [13]. Thus, PV solar projects have the capacity to make a significant contribution to mitigating climate change [14]. Nevertheless, the sensitivity of these systems to atmospheric conditions and future climate variations introduces uncertainty, which can pose challenges to energy planning and potentially impact the effectiveness of PV systems. This uncertainty may hinder investments in the PV energy sector [15, 16].

When contemplating the implementation of a photovoltaic plant, it becomes crucial to assess the future renewable resources rather than solely relying on present conditions, particularly when long-term investments are involved [6]. This forward-looking approach allows for a more comprehensive evaluation of the renewable energy potential and ensures that the investment aligns with long-term sustainability goals. In general, climate change projections are necessary to establish possible future scenarios in order to create subsidies for the development of GHG reduction strategies [17].

In view of the growing concern about the future climate, climate models have been developed. The first general circulation model was developed at Fluid Dynamics Laboratory of the National Oceanic and Atmospheric Administration (NOAA) at the end of the 1960s in Princeton, USA. This model took into account the interactions between oceanic and atmospheric processes and how climatic factors influenced climate change [18]. Currently, global (GCMs) and regional (RCMs) climate models are the main tools used to generate future climate data from a number of parameters, such as air temperature, solar radiation, among others [19, 20].

Within this theme, although there are several studies [15, 21-31] assessing the impacts of climate change on meteorological variables that influence PV energy production, they did not thoroughly examine the impact of these changes on photovoltaic production (P_{pv}).

Several studies have attempted to examine the literature concerning the assessment of climate change's impact on PV energy production. Antonanzas *et al.* (2016) [32] focused on recent research related to solar energy forecasting, but they did not extensively explore PV energy forecasting models. On the other hand, Gandomanin *et al.* (2016) [33] conducted a review of short-term forecasting of PV solar energy production with an emphasis on cloud cover influence. Wan *et al.* (2015) [34] and Raza *et al.* (2016) [35] investigated various PV and solar forecasting techniques but did not specifically address studies utilizing climate models.

Numerical methods have been recently reviewed by Das *et al.* (2018) [36], by Sobri *et al.* (2018) [37] and by Akhter *et al.* (2019) [38], who also did not thoroughly examine climate methods. Numerical methods are based on historical data and on the capacity to extract information from data to predict time series. They include methods based on Statistical Approaches (SA), machine learning techniques (MLT) and hybrids that combine the two previous methods.

Thus, the present study seeks to identify the main results related to the impacts of climate change (ICC) on the P_{pv} from the perspective of climate models. A comprehensive and rigorous approach will be employed to conduct a literature review, aiming to establish correlations between future PV production and its susceptibility to climate change on both regional and global scales. The findings of this research will provide valuable insights for PV energy companies and policymakers to facilitate the planning of the future energy system. The subsequent sections of this paper are structured as follows: Section 2 outlines the methodologies utilized in conducting the scoping systematic review; Section 3 presents an analysis of the literature review, focusing on the effects of climate variability and change (CVC); Section 4 offers a comprehensive discussion, summarizing the findings, identifying research gaps, and assessing the strengths and limitations of the scoping systematic review; and finally, Section 5 provides the conclusion of the study.

2. MATHODOLOGY

Cluster and content analyses were used, which described and interpreted the knowledge and data presented in the papers, and reviewed the content of the selected papers, meeting specific criteria of reliability and validation [39]. The stages of methodological development are described in Figure 1.

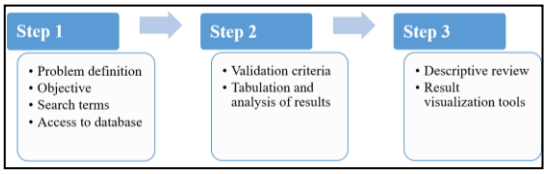

Figure 2: Descriptive summary of the methodological procedure employed.

SStep 1 - Inputs

At first, it was necessary to define the question that will guide this review: *What are the characteristics, amplitude and results of existing research conducted on the impacts of climate change on photovoltaic production from the perspective of simulations using climate models?*

At this point, we sought to estimate the relevance of the problem to be analyzed, in addition to defining the object of study. Subsequently, an exploratory analysis was carried out on how the examination and analysis of climate change effects on photovoltaic production are addressed in the literature. The main words adopted in the articles to define search terms were also identified, based on Emodi *et al.* (2019) [40].

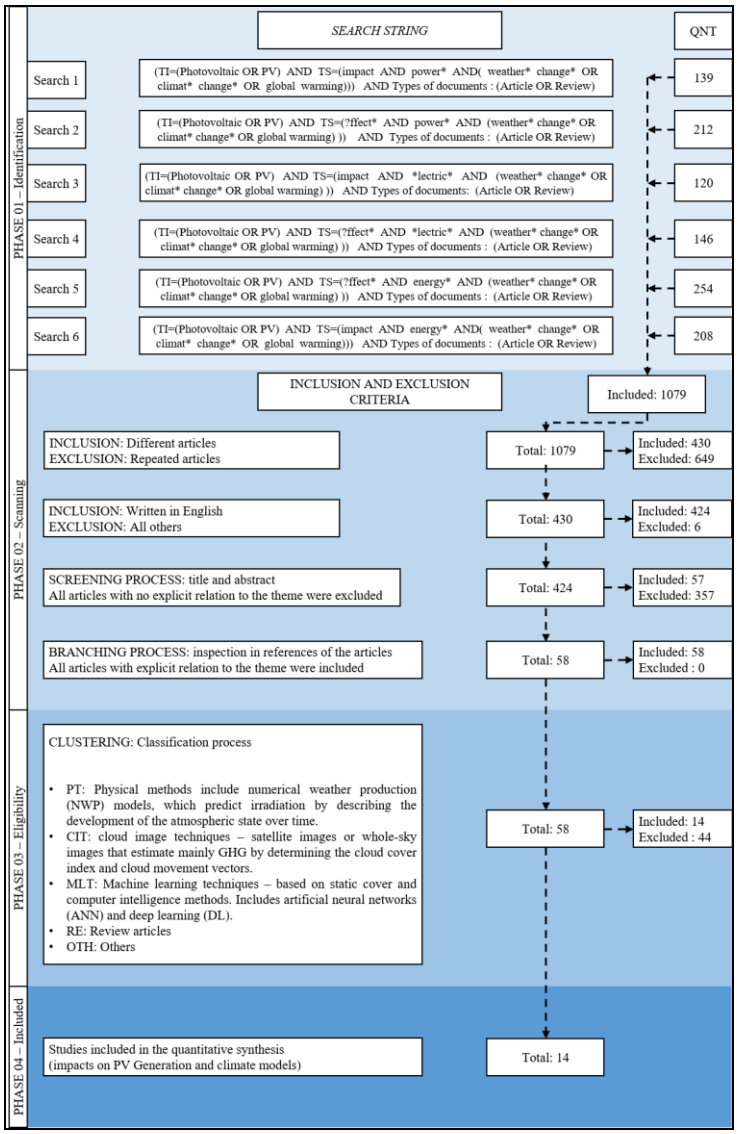

Figure 1: Description and refining of the search for bibliographic references used in the study.

Step 2 - Processing

This stage of the study refers to the definition of the portfolio, described in detail to enable replication of the method. Its construction was based on the preparation of search networks delimited by the theme of the study [40].

Thus, searches were carried out on the Web of Science (WOS) platform, one of the world's most prestigious databases [41], through terms considered relevant by the authors regarding the analysis of the impacts of climate change on PV energy production, as shown in Figure 2. Papers published until 12/31/2023 were included.

The first phase of the research described the process of investigating journals related to the keywords. The terms used were divided into TI ("title") and TS ("topic"). This chosen structure intended to bring the "titles" as the central figure of the search and correlate them with the "topics". The incomplete terms used in the search, such as "*Climat*", plus "*", represent a form of search where the database returns the results of the variations of the term: "*Climate*", "*Clime*" and "*Climatic*". The terms with "*question mark*" (?) used in the search, as in "*?ffect**", represent a form of search where the database returns results with variation of a single letter: "*affect*", "*affected*" and "*effect*".

The second phase comprised the inclusion and exclusion criteria operated for the selection of studies, as observed in Figure 2. First, at the WOS database, only scientific and review articles were chosen. Then, still on the WOS platform, all articles that were repeated and written in a language other than English were excluded. After this previous selection, which generated a considerable number of papers, the screening process was carried out, where the titles and abstracts of all articles were read, and those outside the scope of the study were excluded and all the articles referenced by those already selected that had an explicit relation to the theme were included, a process called branching.

The third phase, characterized by the clustering process, classifies them according to the thematic axis, by content analysis, referring to the pillar (s) of the methodology of analysis and forecasting of PV energy production (PT, CIT, MLT, RE and OTH, Figure 2). Related terms were used to assist in the affinity of inclusion in each category [40]. Considering the objective of this study, the articles that used climate models to qualitatively and quantitatively evaluate the impacts of climate change on PV production were considered eligible.

Data processing was performed in Excel 2013 software [42], by feeding it with information to construct graphs and tables that assisted in the quantitative and qualitative analysis of the articles. The necessary elements were provided by the WOS database itself, such as: title, authors, keywords, number of citations, abstract, year, country and journal of publication.

Step 3 - Outputs

Quantitative and qualitative balances supported a better understanding of the analyzed articles. A scoping review was employed to systematically analyze the existing literature, identifying crucial concepts in the research, evidence types, and sources. This comprehensive approach aids in formulating policies and guiding further research endeavors [40].

3. CHARACTERISTICS OF THE SYSTEMATIC REVIEW ARTICLES

3.1 Main articles

Following the methodology described in Section 2 (Figure 2): in the first phase, a total of 1,079 articles were included; in the second phase, after eliminating repeated papers, those written in a language other than English, and with title and/or abstract with a subject different from the focus of the present study, and evaluating the references, only 58 articles remained; finally, in the third phase, after detailed analysis of the content, a total of 14 articles were extracted. All fourteen articles [5, 6, 16, 43-53] used climate models to quantitatively assess the impacts of climate change on PV energy production over a very long-term horizon.

3.2 Climate models used

According to Diagne *et al.* (2013) [54], climate models can be categorized into three types: global (covering the whole Earth), mesoscale (covering a part of Earth), and regional (focused on specific local regions). Global Climate Models (GCMs) are the main instruments employed for large-scale climate modeling, capable of generating reasonable outcomes on extensive spatial and temporal scales [55]. However, due to their low resolution (both spatial and temporal), GCMs have limitations when it comes to precise evaluations on a regional scale [52].

Regional Climate Models (RCMs) are the answer to overcome these limitations [47]. RCMs offer an enhanced resolution in both temporal and spatial aspects, enabling a more accurate representation of mesoscale atmospheric processes under present and future climate conditions [56, 57, 58]. RCMs face a significant drawback due to the presence of substantial uncertainties in their projections. Climate change research primarily attributes these uncertainties to various factors, including the techniques employed to impose boundary conditions on RCMs, the downscaling methods adopted, and the greenhouse gas emission scenarios utilized [59].

The global and regional climate models used in the forecast of PV production are presented in Tables 1, 2 and 3. Division into three tables was performed

to better arrange the data. From the tables it is possible to notice that Crook *et al.* (2011) [43] were the forerunners in this line of research. The authors conducted an investigation into the potential impacts of solar temperature and irradiation changes on the generation of PV energy and concentrated solar power (CSP) throughout the 21st century. To accomplish this, they obtained projected climatic data from two GCMs. In their study, Crook *et al.* (2011) [43] emphasized the importance of conducting similar analyses using a broader range of climate models to enhance comprehension of the variability in energy production due to uncertainties in solar irradiation projections. The initial findings presented by the authors can be regarded as a preliminary estimation of magnitude.

3.2.1 Entire globe

A total of six works used climate models to analyze the ICC-P_{pv} at the level of China or the entire globe (Table 1). Due to the fact of analyzing the future from models, which have numerous uncertainties, it is verified in Table 1, as expected, that the works use more than one GCM model to carry out the analyzes of the magnitude and consistency of the ICC-P_{pv} a world level. The works by Wild *et al.* (2015) [46] and Zou *et al.* (2019) [51] used, respectively, 39 and 37 global models from CMIP5 (2013) [60], while Feron *et al.* (2021) [16] used 7 models; Crook *et al.* (2011) [43], 2 models; Zhao *et al.* (2020) [5], 3 models; and Smith *et al.* (2017) only one GCM.

In a comparative study of 14 models from the Coupled Model Intercomparison Project Phase 3 (CMIP3), the HadCM3 model was recognized as one of the top-performing models for global average annual insolation under clear skies. However, it is important to note that this study did not include HadGEM1 [61]. When taking HadGEM1 into account, it becomes evident that it slightly outperforms HadCM3 and holds greater potential for accurately reproducing future changes. This is due to HadGEM1's inclusion of a more advanced and physically-based aerosol modeling approach [43]. It can be seen in Tables 1, 2 and 3 that Crook *et al.* (2011) [43] were the first and last to use the HadGEM1 family of climate models, and the later works [6,46,47,52,53] used the next version developed by the UK Metrology Office (Metrology Office UK) (HadGEM2).

In the simulations performed by Smith *et al.* (2017) [50] with the HadGEM2-CCS model under RCP4.5 and employing the geoengineering method, Stratospheric sulfate injection (SSI), in the period of 2040-2059, the authors analyzed the ICC-P_{pv}.

Zhao *et al.* (2020) [5], different from previous studies, projected the future climate over China using stepwise cluster analysis (SCA). SCA was shosen as a downscaling technique to downsize GCM forecasts based on Huang (1992) [62] and Wilks (1932) [63]. Zhao *et al.* (2020) [5] were the first ones to consider improvement rates for the absolute efficiency of PV technology (range of 0.04–0.09% per year).

Until then, studies had focused on the ICC-P_{pv} analysis based on average projection results, however, Feron *et al.* (2021) [16] concentrated on examining the impacts of atypical weather conditions and extreme weather events on PV outputs. An important conclusion was that changes in the frequency of these unusual weather conditions can increase or reduce the intermittency of P_{pv}, with consequences for network planning and operations.

3.2.2 European continent

When analyzing Table 2, it is observed that there is no unanimity about which are the best sets of models (GCMs and RCMs) to analyze the European continent, in fact, there is a great variability among the five works identified. Three of the five papers, however, use at least five different RCM/GCM sets to carry out analyzes of the magnitude and consistency of ICC-P_{pv} in Europe. The GCMs that were used in at least two works were ECHAM5, EC-EARTH, HadGEM2-ES and IPSL-CM5A-MR. The only RCMs that were used in more than one work are HIRHAM5 (v2) and WRF.

A distinctive feature was identified in the study conducted by Jerez *et al.* (2015b) [47], where they examined, considering a future scenario characterized by a significant penetration of PV installations, the ICC-P_{pv} at the level of European regional electric grids. The optimal distribution of installed PV power across the region was obtained using the CLIMIX model. [64]. In addition, Gaetani *et al.* (2014) [45], besides investigating the ICC-P_{pv} in Europe, the Eastern Mediterranean and Africa, observed the influence of factors such as aerosols, cloud cover, temperature. Additionally, within the framework of the enviroGRIDS project of the 7th Framework Programme of the European Union, Lehmann *et al.* (2015) [65] and Gunderson *et al.* (2015) [48] carried out research with a particular focus on the Black Sea region.

Pérez *et al.* (2019), that used Weather Research and Forecasting (WRF) model [66] as RCM, argued that the use of reanalysis data is one of the main usefulness of the PGW (see subsection 4.3.5), since the tendencies in the border conditions, with regard to genuine meteorology, are much smaller [67].

Table 1 – Climate models used by articles that analyzed China or the entire globe.

GCM	Articles
ACCESS1.0	[46], [51]
ACCESS1.3	[16], [46], [51]
BNU-ESM	[46]
BCC-CSM1.1	[46]
BCC-CSM1.1(m)	[46]
CanESM2	[16], [46], [51]
CanCM4	[51]
CCSM4	[46], [51]
CESM1-BGC	[46]
CESM1-CAM5	[46], [51]
CESM1-WACCM	[46]
CMCC-CESM	[46], [51]
CMCC-CMS	[46], [51]
CMCC-CM	[46], [51]
CNRM-CM5	[5], [46], [51]
CNRM-CM5-2	[51]
CSIRO-Mk3.6.0	[46], [51]
CSIRO-Mk3L.1.2	[51]
EC-EARTH	[46]
FGOALS-g2	[46]
FGOALS-s2	[46], [51]
FIO-ESM	[46]
GFDL-CM3	[46]
GFDL-ESM2G	[46]
GFDL-ESM2M	[16], [46]
GISS-E2-H	[46], [51]
GISS-E2-H-CC	[51]
GISS-E2-R	[46], [51]
GISS-E2-R-CC	[51]
HadCM3	[43], [51]
HadGEM1	[43]
HadGEM2-AO	[46], [51]
HadGEM2-CC	[46], [51]
HadGEM2-CCS	[50]
HadGEM2-ES	[46], [51]
INM-CM4	[5], [16], [46], [51]
IPSL-CM5A-LR	[46], [51]
IPSL-CM5A-MR	[46], [51]
IPSL-CM5B-LR	[46], [51]
MIROC5	[46], [51]
MIROC4h	[51]
MIROC-ESM-CHEM	[16], [46], [51]
MIROC-ESM	[51]
MPI-ESM-LR	[5], [16], [46], [51]
MPI-ESM-MR	[46], [51]
MPI-ESM-P	[51]
MRI-CGCM3	[16], [46], [51]
MRI-ESM1	[51]
NorESM1-ME	[46], [51]
NorESM1-M	[46], [51]

Table 2 – Climate models used by articles that analyzed a country, a region or the entire Europe.

GCM\RCM	HIRHAM5 (v2)	RACMO22T (v1)	RCA4 (v1)	REMO2009 (v1)	CCLM4-8-17 (v1)	ALADIN	C4IRCA3	ETHZ-CLM	MPI-M-REMO	SMHIRCA	CNRM-RM5.1	WRF
APREGE RM5.1											[44]	
BCM										[44]		
CSIRO-Mk3.6.0												[6]
CCSM4												[6]
CNRM-CM5			[48]									
ECHAM5	[45]								[44]			
EC-EARTH	[48]	[48]	[48]									[6]
GFDL-ESM2G												[6]
HadCM3Q0								[44]				
HadCM3Q16							[44]					
HadGEM2-ES			[48]		[48]							[6]
HadAM3H	[48]											
INM-CM4												[6]
IPSL-CM5A-MR			[48]									[6] [48]
MIROC5												[6]
MPI-ESM-LR			[48]	[48]								

Table 3 – Climate models used by articles that analyzed a region or the entire Africa.

GCM\RCM	None	HIRHAM5 (v2)	RACMO22T (v1)	RCA4 (v1)	REMO2009 (v1)	CCLM4-8-17 (v1)	ALADIN	NOAA	NCC	MPI	MIROC	IPSL	ICHEC	CNRM	CCCMA
CanESM2				[52], [53]											[49]
CNRM-CM5				[52], [53]		[52], [53]	[53]							[49]	
CSIRO-Mk3.6.0				[52], [53]											
EC-EARTH		[52]	[52], [53]	[52]	[52]	[53]							[49]		
ECHAM5	[45]														
GFDL-ESM2M				[52]				[49]							
HadAM3H															
HadGEM2-ES			[52]	[52], [53]		[53]									
IPSL-CM5A-MR				[52], [53]								[49]			
MIROC5				[52], [53]							[49]				
MPI-ESM-LR				[52], [53]	[52]	[52], [53]				[49]					
NorESM1-M				[52], [53]					[49]						

3.2.3. African continent

The most common justification for analyzing this part of the world lies in the region's solar potential [49].

When the studies are at the level of the African continent (Table 3), it is observed that two of the four works used quite a lot of GCM/RCM sets in common, while the other two analyze the impact from sets that are very different from each other. The works of Bichet *et al.* (2019) [52] and Sawadogo *et al.* (2020) [53] complement each other. Both used the results of CORDEX-AFRICA, which was the most up-to-date for Africa [52].

Bichet *et al.* (2019) [52], in addition to Bazyomo *et al.* (2016) [49] also evaluated the P_{pv} and its response to meteorological variance throughout the Africa. Besides, they estimated the overall uncertainty related to these forecasts and to the distinct uncertainty origins: inherent variability and the uncertainty due to the use of climate models.

Bazyomo *et al.* (2016) [49], unlike previous studies [43,46], calculated solar irradiation on a tilted plane from daily data of total sky radiation with the free R package, the solaR [68].

3.3 Emission scenarios used

Climate researchers employ socioeconomic and emission scenarios to present realistic depictions of future developments concerning various factors, such as socioeconomic changes, technological advancements, energy and land use, greenhouse gas emissions, and air pollutants. These scenarios serve as inputs for climate models, facilitating assessments of potential climate impacts, mitigation strategies, and their associated costs. For improved comparability between studies and enhanced communication of model outcomes, it is essential for the entire scientific community to adopt a standardized set of scenarios [69].

From Table 4, it can be observed that the set of SRES scenarios was used until 2015; from that year onwards the more current models, the RCPs, became the only ones used during the PV production forecasting process. RCP4.5 [70] and RCP8.5 [71] are the emission scenarios most frequently utilized in climate forecasts [5]. The most frequently utilized scenario in the research was RCP8.5, which is commonly employed in the literature to depict high concentrations of greenhouse gases. This scenario ensures a higher signal-to-noise ratio, making it easier to identify distinct patterns of change in climate [46].

In addition to emission scenarios, there are still some methods that are coupled, such as pseudo-global warming (PGW) [67,72,73]. The application of PGW seeks to reduce the computational charge related to High resolution in space and extended data collection periods by using shorter simulation periods [74,75], instead of periods of three decades or more [76].

Table 4 - Emission scenarios used in ICC-P_{pv} studies.

Paper	Emission scenarios				
	SRES A1B	SRES A2	SRES B2	RCP4.5	RCP8.5
[5]				X	X
[6]				X + PGW	X + PGW
[16]				X	X
[43]	X				
[44]	X				
[45]			X		
[46]					X
[47]				X	X
[48]		X	X		
[49]					X
[50]				X	
[51]					X
[52]					X
[53]					X + PGW

X + PGW: used the indicated emission scenario, associated with the pseudo-global warming (PGW) technique.

Furthermore, Sawadogo *et al.* (2020) [5] adopted a different approach, selecting global warming levels (GWL) above the pre-industrial level (PI) (1881-1910). To determine the 30-year GWL for each Global Climate Model (GCM) simulation, they considered a 30-year period centered on the year when the GCM reaches 1.5, 2.0, 2.5, and 3.0 °C in Global Mean Temperature (GMT) compared to PI levels under RCP 8.5 [77]. The analysis involved using the same GWL period of the GCM to extract the 30 years of GCM data, which were then reduced by the Regional Climate Model (RCM) using 1971-2000 as a control period.

3.4 Databases used

Table 5 shows the databases used by the articles that assess ICC-P_{pv}. With the exception of Gunderson *et al.* (2015) [48], all the others used data from either CMIP or CORDEX.

The CMIP3 and CMIP5 initiatives offer a standardized platform for studying and comparing global coupled atmosphere-ocean models (AOGCMs) through structured experiments [78]. These experiments formed the foundation for evaluating the 4th and 5th Reports of the Intergovernmental Panel on Climate Change [79]. In CMIP5 an in CMIP3, predefined scenarios of radiative forcing were used for climate change projections [80]. The newly developed CMIP6 [81] has not yet been used in ICC-P_{pv} studies.

One of the largest and most recent databases in constant updating is that of the Coordinated Regional Climate Downscaling Experiment (CORDEX) [82], which seeks to promote and synchronize scientific research and the utilization of regional climate downscaling through international collaborations [83]. It provides a framework for investigating the scenarios of impact of climate change on a regional scale [84]. There is a total of fourteen official CORDEX domains. The CORDEX-EUROPE covers Europe with a spatial resolution of 0.11° in latitude and longitude, and provides records of output variables every 3 hours. CORDEX-AFRICA simulations cover all Africa with a spatial resolution of CORDEX data sets of approximately 50 km (0.44° x 0.44°). For each simulation and each grid cell, many meteorological variables are available. From the CORDEX data sets, it is possible to obtain average daily surface downwelling shortwave radiation (G_{tot}; also called solar irradiance), air temperature (T_a), wind speed (W; at 10 m above ground level) and relative humidity (R_h).

Sawadogo *et al.* (2020) [53] used the ERA-Interim reanalysis data set of the European Centre for Medium-Range Weather Forecast (ECMWF). On the website of ECMWF, they retrieved the surface wind speed (10 m above ground level) and the relative humidity that was calculated from the dew point and the specific humidity.

Some authors used data analysis with the R programming language to analyze the solar radiation values extracted from RCM [48]. Gunderson *et al.* (2015) [48] also applied common kriging interpolation to create a solar radiation surface and considered the topographic effects of aspect and inclination on solar radiation by incorporating a solar indexation layer that considered the relative difference in incident solar irradiation based on its alignment or positioning and angle of arrival.

Pérez *et al.* (2019) [6] utilized information from on-site measuring devices and two data repositories, satellite-based information, to evaluate simulated outcomes for the past time frame. This type of decision is very recurrent and it is commonly motivated by the significant spatial diversity of irradiance in the investigation region.

3.5 Data extraction methods

3.5.1 Irradiance - Interpolation

Precise understanding of solar irradiation in a particular region is essential, especially for applications in solar energy resources [85]. Various factors can lead to significant local gradients of solar irradiance over small distances, such as changes in height, positioning, incline, shadows, and surface reflectivity [86,87]. Studies concur that topography plays a significant role on a local scale and should be taken into account when considering solar systems' proper location [88,89].

Table 5 - Database used in papers in ICC-P_{pv} studies.

Paper	Air temperature	Solar irradiation	Wind Speed	Relative humidity
[5]	CMIP5; ERA-Interim; National Meteorological Information Center of China	CMIP5; ERA-Interim; National Meteorological Information Center of China	-	-
[6]	project ADRASE AEMET CMIP5	SoDa service AEMET CMIP5	AEMET CMIP5	-
[16]	CMIP5	CMIP5	CMIP5	-
[43]	CMIP3	CMIP3	-	-
[44]	E-OBS CORDEX-EUROPE	SoDa service CORDEX-EUROPE	-	-
[45]	FP6-EUCAARI project	FP6-EUCAARI project	-	-
[46]	CMIP5	CMIP5	-	-
[47]	CORDEX-EUROPE	CORDEX-EUROPE	CORDEX-EUROPE	-
[48]	-	PRUDENCE NCEP/NCAR	-	-
[49]	CORDEX-AFRICA	CORDEX-AFRICA	-	-
[50]	CMIP5	CMIP5	-	-
[51]	CMIP5	CMIP5	-	-
[52]	CORDEX-AFRICA	CORDEX-AFRICA	CORDEX-AFRICA	-
[53]	CORDEX-AFRICA CRU	CORDEX-AFRICA SARAH-2	CORDEX-AFRICA ECMWF website	CORDEX-AFRICA ECMWF website

Solar irradiance plays a crucial role in various terrestrial processes, and in situations where direct measurements are unavailable, alternative techniques are necessary to evaluate the solar potential [90]. Interpolation is one such effective method for estimating local and temporal components of solar irradiance when whether data is lacking, allowing for the creation of spatially continuous databases across large regions [87,88]. However, the reliability of interpolation decreases in areas with complex topography, and its accuracy significantly relies on the database size and the spacing between stations [87-90]. In order to enhance the precision and dependability of spatial interpolation for solar irradiation on a local scale, topographic variables are often integrated, utilizing digital elevation models (DEM) [86-90].

3.5.2 Daily temperature and irradiance – sinusoidal form

Crook *et al.* (2011) [43] assume that climate data are average during the day and night, that is, they vary approximately sinusoidally, but only temperatures and solar irradiance during the day are required to estimate PV energy production. In order to account for the average monthly diurnal temperature (T_{day}), Crook *et al.* (2011) [43] proposed an adjustment method based on the assumption of a sinusoidal temperature variation throughout the day. They considered a range equal to half of the diurnal temperature range (DTR), which signifies the disparity between the highest and lowest temperatures within a day, as well as an average

value denoted as $\overline{T}$. By applying this approach, they approximated T_{day} as follows:

$$T_{day} = \overline{T} + \frac{DTR}{4} \quad (1)$$

The notation of a bar indicates monthly averages in the following passage. The selected models did not provide maximum and minimum temperatures. Hence, historical climatological diurnal temperature range (DTR) data for each month from some data set can be utilized. It was assumed that the DTR would remain constant in future scenarios, although there is a lack of consensus regarding potential changes in DTR in the future. [91]. The average solar irradiance during the hours when sunlight is available for operation should be estimated based on the duration of the day:

$$G_{day} = \overline{G} + \frac{t_{24h}}{t_{duration\ of\ the\ day}} \quad (2)$$

Here, $\overline{G}$ represents the monthly average of G_{tot} when specifically considering photovoltaic energy. The duration of daylight is once again employed in the calculation of energy production for every month.

3.5.3 Solar irradiance from the duration of insolation

In some situations, daily solar irradiance (DSI) is not available throughout the desired period, but the daily duration of insolation (DDI) is available. For this reason, Pérez *et al.* (2019) [6] used a method to transform the DDI into DSI, using the association identified in earlier researches [22, 92]. This association can be stated as:

$$f_{clear} = \left(\frac{\overline{G}_{total}}{\overline{G}_{clear}} \right)^2 \quad (3)$$

in the given equation, f_{clear} denotes the fraction of clear sky time, $\overline{G}_{total}$ represents the monthly average of daily horizontal surface irradiation and $\overline{G}_{clear}$ stands for the average daily irradiation value with clear sky. This fraction, specific to a particular month and location, corresponds to the proportion of sunlight (S):

$$f_{clear} \equiv S = \frac{DSL}{DD} \quad (4)$$

associated with the following equations:

$$DD = \frac{2}{15}\cos^{-1}(\tan\phi \tan\delta) \quad (5)$$

$$\delta = 23.45 \sin\left(360 \frac{284 + n}{365} \right) \quad (6)$$

where DSL is the average monthly duration of sunlight, DD is the average monthly duration of the day, ϕ is the latitude of the place in degrees, δ is the declination of the sun, also in degrees, n is the day of the year, starting on January 1.

Thus, for a given location and month, $\bar{G}_{tot}$ can be calculated as:

$$\overline{G}_{total} = \overline{G}_{clear} \left(\frac{DSL}{DD} \right)^{1/2} \quad (7)$$

In cases where $\overline{G}_{clear}$ is not directly obtainable from observational data, an alternative approach involves deriving it for each location and specific month of the year by utilizing available data on daily horizontal surface radiation and sunlight duration from recent years. Once the values for $\overline{G}_{clear}$ are determined, solar irradiance can be calculated for any desired month.

According to Pérez *et al.* (2019) [6], employing this methodology leads to a root mean square error of 3.3% when comparing the calculated $\overline{G}_{total}$ with the observed values.

3.6 Methodologies used for bias correction

The methodology for the correction approach is dependent on several factors, such as the nature of the data, the time frame, the spatial and temporal resolution, and the time frame considered [44]. To handle inconclusiveness arising from various potential outcomes of the meteorological system, sets of climate model outputs can be employed. Multiple global climate models (GCMs) can be employed to assess uncertainty associated with different large-scale physical parameterizations of terrestrial and atmospheric processes. Additionally, the utilization of different regional climate models (RCMs) can help address uncertainties associated with the depiction of smaller-scale phenomena, such as microphysical clouds or convective rainfall.

A number of GCMs exhibit notable biases when it comes to accurately representing the absolute levels of G_{total} [93] and T_a [94] in comparison to surface observations. These discrepancies are often attributed to challenges related to parameterizing cloud effects [95], as well as shortcomings in clear sky radiation modeling (WILD *et al.*, 2006) [61].

RCMs often exhibit variations in the statistical characteristics of simulated meteorological

data when compared to observed values. A prominent component of this temporal error is the presence of bias [96]. To align the outputs of climate models with the prevailing climate conditions, it becomes necessary to employ bias correction techniques. Various studies, including Haerter *et al.* (2011) [96], Christensen *et al.* (2008) [97], Terink *et al.* (2009) [98], and Boberg and Christensen (2012) [99], emphasize the importance of bias correction to ensure that impact models, particularly in hydrology, water resource management, and other climatic applications, generate meaningful and reliable results.

In their study, Panagea *et al.* (2014) [44] implemented a correction process for temperature and irradiance projections to account for biases in the mean and standard deviation on a monthly basis. This methodology was derived from the approach presented by Haerter *et al.* (2011) [96] and was applied prior to the conversion of projections into PV energy production. The mean bias was addressed by calculating differences from observed and modeled values. Subsequently, the model data is consistently normalized according to the variability observed in historical data. When the data exhibits a normal distribution, the transfer function adheres to a linear relationship as expressed in the following equation:

$$X_{sc}^{cor} = \left(X_{mod}^{sc} - \bar{X}_{mod}^{con}\right)\left(\frac{\sigma_{obs}^{con}}{\sigma_{mod}^{con}}\right) + \bar{X}_{obs}^{con} \qquad (8)$$

X_{sc}^{cor} represents the final adjusted time series, X_{mod}^{sc} denotes the "raw" model forecasts for the scenario period, X_{obs}^{con} and X_{mod}^{con} represent the averages of observed and modeled data for the control period, respectively, σ_{obs}^{con} and σ_{mod}^{con} refer to the standard deviations of observed and modeled data for the control period, respectively.

The assessment of the impact of systematic biases on irradiance and temperature levels in the projected changes of P_{pv} is very important, and it has already been conducted [46]. To assess the sensitivity, it can be performed by altering the input levels of G_{tot} and T_a within a range of ± 10 W/m2 and ± 10 °C. The existing findings revealed that these changes did not exert a significant influence on the projected absolute values of P_{pv} [46]. This suggests a low sensitivity of the utilized methodology to the absolute levels of these meteorological variables across all focal regions examined, namely Algeria, Australia, California, Northwest China, Germany, India, South Africa, and Spain. Consequently, unlike Panagea et al. (2014) [44], Wild et al. (2015) [46] did not utilize bias corrections on the simulated temperature and irradiance fields before computing P_{pv}.

It is important to mention that all the alterations described in Wild *et al.* (2015) [46] are related to representative changes for horizontal planes, as inferred from the output of the climate model. Nonetheless, variations in solar radiation on tilted or tracked planes (planes positioned perpendicular to the sunbeam) generally exhibit greater magnitudes. For instance, in Germany, Müller *et al.* (2014) [100] found that changes on tracked planes can be more than double the corresponding variations on horizontal planes.

In their study, Zhao *et al.* (2020) [5] employed a filtering process on the ERA-Interim reanalysis variables [101]. These variables served as potential predictors to establish the connection between the circulation of the atmosphere on a large scale and the local weather parameters. The purpose of the filtering was to remove uncorrelated variables, thereby reducing the computational load associated with the analysis.

The assessment of time variability across different scales, including daily, monthly, and annual time scales, can be conducted [47]. This allowed the highlighting of an important consideration to prevent the masking effect of the annual PV production cycle. To address this, the removal of the multiannual monthly and daily averages from the corresponding monthly and daily series can be performed. This step will aim to ensure a more accurate representation of the underlying variability and avoid potential distortions caused by the annual production cycle.

Bazyomo *et al.* (2016) [49] presented their findings based on annual averages of temperature and irradiation. To calculate these averages, they utilized the Climate Data Operators [102], with daily data as input. Subsequently, they employed the free software R [103] to compute all the averages. Subsequently, the values were resampled to ensure uniform resolution. The determination of patterns and their statistical significance were computed using the Stats package within R. Following the approach employed by Jerez *et al.* (2015b) [47], only cells corresponding to $p \leq 0.05$ values were retained by utilizing the Student's t-test.

A moving block bootstrap algorithm as a method to account for the effects of data autocorrelation was employed by Pérez *et al.* (2019) [6]. This approach incorporated an autoregressive moving average process, building upon previous evaluations of this method as demonstrated by Expósito *et al.* (2015) [104] and González *et al.* (2017) [105]. Additionally, the block length for the bootstrap test and the adjustment of data variance for the test statistic were computed following the methodology outlined by Wilks (1997) [106].

R_{mean} is created by combining multiple models with equal weights and has been observed to exhibit better performance compared to any individual model [107, 108]. It is generally regarded as having superior overall performance compared to

an individual model [109]. Furthermore, R_{mean} yields improved outcomes when it comes to long-term climate change projections compared to using only an individual model [110].

3.7 Methodologies used to quantify uncertainties

Bichet *et al.* (2019) [52] sought to quantify the uncertainties of:

i. The climate models: due to its imperfections; and
ii. The inherent climatic variability, arising from the unsteady and nonlinear behavior of the meteorological system.

The partitioning and quantification of various sources of uncertainty can be accomplished using QUALYPSO [111], which is an advanced ANOVA Bayesian method [112].

3.8 Simulation periods used

Table 6 shows the reference periods and those projected by the papers. It is observed that, for the most part, they analyzed until the end of the XXI century, and only about 20% [16, 46, 49] analyzed until the mid-21st century.

In their study, Sawadogo *et al.* (2020) [53] emphasized the challenge policymakers may face when attempting to apply projection results to the specific warming levels (1.5 °C and 2.0 °C) required by the Paris Agreement. To address this issue, they advocated for the adoption of global warming levels (GWL) in comparison to the period before industrialization (1881-1910). Specifically, they considered positive anomalies of 1.5 °C, 2.0 °C, 2.5 °C, and 3.0 °C as their chosen GWL values. This approach enables policymakers to have more relevant information for decision-making within the context of the Paris Agreement.

It is common practice to designate the initial year as a spin-up period, which is not included in any subsequent analysis, as it was done by Pérez *et al.* (2019) [6].

3.9 Methodologies used in ICC-P_{pv} analysis

PV energy yields depend on shortwave irradiance, which in turn is modulated by aerosols [113-115] and by clouds [116]. PV outputs are also affected by air temperature (T_a), with an inversely proportional ratio [117]. Surface wind velocity (ν) also influences PV production, as airflow usually cools the PV module [118].

The efficiency of a PV cell as a function of cell temperature and radiation can be expressed by an established linear ratio with a negative gradient.

$$\frac{\eta_{cell}}{\eta_{ref}} = 1 - \beta(T_{cell} - T_{ref}) + \gamma \log_{10} G_{tot} \qquad (8)$$

in the given equation, η_{ref} represents the reference efficiency, while β and γ denote the coefficients of temperature and irradiance, respectively. These coefficients are specific to the cell material and structure being used. Additionally, T_{cell} represents the cell temperature, and T_{ref} corresponds to the reference temperature [119-120].

The decrease in efficiency of PV silicon at low-light levels is taken into consideration through γ [121]. According to Crook *et al.* (2011) [43], for monocrystalline silicon cells, $\beta = 0.0045 / {}^{\circ}C$ and $\gamma = 0.1$, and $T_{ref} = 25^{\circ}C$ should be used.

Table 6 - Reference periods and projected periods analyzed in the papers.

Paper	Reference periods	Projected periods
[5]	1981-2005	2020-2039, 2040-2069 and 2070-2099
[6]	1995-2004	2045-2054 and 2090-2099
[16]	1961-1990	2036-2065
[43]	1980-1999	2010 to 2080
[44]	Temperature: 1950-2000 Irradiation: 1985-2005	2011-2050 and 2061-2100
[45]	2000	2030
[46]	2006-2015	2006-2049
[47]	1970-1999	2070-2099
[48]	1961-1990	2071-2100
[49]	2006-2015	2006-2045
[50]	1860-2005	2006-2099
[51]	1850-2005	2006-2100
[52]	1995-2005	2070-2099
[53]	1971-2000	GWL 1.5, 2.0, 2.5, 3.0

The value of η_{ref} holds no significance if only considered the fractional change in photovoltaic production, $\Delta P_{pv} / P_{pv}$ is considered in the analysis. It is worth noting that minor errors may arise due to the nonlinearity of G and T in Equation (8) caused by the daily averaging of G and T. A computer-based modeling and simulation conducted under cloudless conditions suggests that these errors vary between

1% to 2%, and their magnitude depends on the latitude [43]. Nevertheless, it is essential to acknowledge that these errors exhibit a systematic pattern and have a negligible influence on the year-to-year percentage variation in P_{pv} [43].

In the sequence of studies of several authors [122-124], a generic empirical formula was established to represent the cell temperature as follows:

$$T_{cell} = c_1 + c_2 T_a + c_3 G_{tot} \quad (9)$$

Where T_a is the ambient temperature in °C. The constants are dependent on module and assembly specifics, which influence cell heat transfer. The coefficients normally used in this equation were extracted from the study of Lasnier and Ang (1990) [122] for a monocrystalline silicon cell, which are: $c_1 = -3.75^{o}C$, $c_2 = 1.14$ and $c_3 = 0.0175^{o}Cm^2/W$. The equation used to calculate PV energy production is:

$$P_{pv} = G_{tot}\eta_{cell} \quad (10)$$

Omar *et al.* (2014) [125] consider, in addition to the terms of Eq. (10), some efficiency reduction factors related to dust, module incompatibility, cabling and inverter. All these factors are intrinsic to the PV system, but not to the PV technology.

The annual energy production is given by:

$$E = \sum_{month} 30 P t_{duration\ of\ the\ day} \quad (11)$$

assuming 30 days for each month.

Panagea *et al.* (2014) [44] and Zhao *et al.* (2020) [5] used the same equations as Crook *et al.* (2011) [43and also used monthly averages. On the contrary, Wild *et al.* (2015) [46] conducted their analyses, including assessments of changes in P_{pv}, using average annual data. As a result, the estimates provided by Wild *et al.* (2015) [46] do not account for potential nonlinear effects attributed to seasonal variations in radiation and temperature changes.

Bazyomo *et al.* (2016) [49] used the same equations (Eq. 8 and Eq. 9) as Crook *et al.* (2011) [43], but, as done by Wild *et al.* (2015) [46], used annual averages from daily data, and considered solar irradiation on the inclined plane calculated with the solaR suite of R [68] utilizing the daily data of total solar radiation as inputs.

Unlike Crook *et al.* (2011) [43] and their successors, Jerez *et al.* (2015a) [47] did not use Eq. (8), but proposed the use of a new equation in accordance with Tonui and Tripanagnostopoulos (2008) [126]:

$$\frac{\eta_{cell}}{\eta_{ref}} = 1 - \beta(T_{cell} - T_{ref}) \quad (12)$$

where now β assumes the value of 0.005/°C for monocrystalline silicon cells [126].

Again, diverging from the methodology of Crook *et al.* (2011) [43] and their successors, Jerez *et al.* (2015b) [47] did not use Eq. (9), but proposed the use of a new equation, now considering the influence of wind speed, according to Chenni *et al.* (2007) [118]:

$$T_{cell} = c_1 + c_2 T_a + c_3 G_{tot} + c_4 W_{10} \quad (13)$$

where W_{10} is the wind speed on the Earth's surface in m/s.

According to Chenni *et al.* (2007) [118], the coefficients for a monocrystalline silicon cell are $c_1 = 4.73^{o}C$, $c_2 = 0.943$ and $c_3 = 0.028^{o}Cm^2/W$ and $c_4 = -1.528^{o}Cs/m$.

Bichet *et al.* (2019) [52], Pérez *et al.* (2019) [6] and Feron *et al.* (2021) [16] used the same equations as Jerez *et al.* (2015a) [47] for daily data. However, Pérez *et al.* (2019) [6] changed the values of the coefficients to $c_1 = 4.22^{o}C$, $c_2 = 1.08$ and $c_3 = 0.0226^{o}Cm^2/W$ and $c_4 = -1.83^{o}Cs/m$ [127]. However, it was shown that this equation is not suitable for W_{10} greater than 10 m/s, as it produces an incompatible temperature for the PV module [6].

Sawadogo *et al.* (2020) [53] used the same Eq. (12) as Jerez *et al.* (2015a) [47], but replaced Eq. (13) with:

$$T_{cell} = c_1 + c_2 T_a + c_3 G_{tot} + c_4 W_{10} + c_5 W + c_5 R_h \quad (14)$$

Where R_h is relative humidity in %.

According to Tamizhmani *et al.* (2003) [128], the system-specific regression coefficients are $c_1 = 1.57^{o}C$, $c_2 = 0.961$ and $c_3 = 0.0289^{o}Cm^2/W$ and $c_4 = -1.457^{o}Cs/m$ and $c_5 = 0.109^{o}C/\%$. In a study by Mekhilef *et al.* (2012) [129], two scenarios were presented to demonstrate the influence of humidity on PV cell performance. The first scenario involves the impact of water vapor particles on solar irradiance, while the second scenario considers the entry of humidity into the solar cell enclosure. The research revealed that increasing relative air humidity can lead to a reduction in P_{pv} performance, as water droplets within the cell can reflect solar irradiance. Conversely, an increase in wind speed has a cooling effect on the cells, thus enhancing PV cell efficiency. Therefore, selecting an appropriate model aid in achieving a more stable cell temperature and facilitates the comparison of additional variables' contributions to cell temperature. Moreover, the last

model (Equation 14) was formulated and validated using on-site measurements of meteorological variables collected from a weather station. TamizhMani *et al.* (2003) [128] demonstrated a correlation greater than 0.9 between the model's results and the observed data.

Unlike all previous studies, Gunderson *et al.* (2015) [48] opted for a simplistic model that adopts:

$$P_{pv} = G_{tot}\eta_{cell} = G_{tot} \cdot 0.15 \quad (15)$$

that is, it does not consider the influence of any environmental factor other than solar irradiation.

Some other relationships to describe the dependence of solar cell temperature on the meteorological variables have been used. Zou *et al.* (2019) [51] used Eq. (16):

$$T_{cell} = T_a + (T_{NOCT} - 20)\left(\frac{G_{tot}}{800}\right) \quad (16)$$

Where T_{NOCT} represents the nominal operating cell temperature, which is characterized as the temperature achieved when cells are installed in a specific location with standard conditions, including a solar radiation level of 800 W/m², wind speed of 1 m/s, and ambient temperature of 20 °C.

Smith *et al.* (2017) [50] used Eq. (17) to define cell temperature:

$$T_{cell} = T_a + c_3 G_{tot} \quad (17)$$

This assumption is based on the installation of the PV module in an open field environment where the impact of free-flowing wind speed on convection heat transfer away from the module is negligible. According to Skoplaki *et al.* (2008) [130], the corresponding coefficient is denoted as c_3 with a value of 0.02933 K/Wm².

Gaetani *et al.* (2014) [45] chose not to utilize the aforementioned equations and instead employed the methodology developed by Huld *et al.* (2010) [131]. This approach involves utilizing a mathematical model that relates the energy performance of PV modules to the irradiance on the plane and module temperature. It combines this model with satellite-derived estimates of solar

irradiation and ground-based measurements of ambient temperature values from weather stations.

It must be clear that the real values of T_{cell} and η_{cell} are slightly different from those calculated due to empirical nature of equations. However, since this proportion will affect P_{pv} in a similar way during the reference and the future period, it has an even smaller effect on the expected relative change in P_{pv} [16].

A synthesis of the equations used is presented in Table 7.

Table 7 - Equations used to estimate the PV production.

Paper	Equations	Primary reference*
[53]	$\eta_{cell}=\eta_{ref}[1-\beta(T_{cell}-T_{ref})]$ $T_{cell} = c_1 + c_2T_a + c_3G_{tot} + c_4W + c_5R_h$	η_{cell}: [148] T_{cell}: [128]
[5] [49] [44] [46] [43]	$\eta_{cell}=\eta_{ref}[1-\beta(T_{cell}-T_{ref})+\gamma\, log_{10}G_{tot}]$ $T_{cell} = c_1 + c_2T_a + c_3G_{tot}$	η_{cell}: [149] and [150] T_{cell}: [122]
[16] [6] [52] [47]	$\eta_{cell}=\eta_{ref}[1-\beta(T_{cell}-T_{ref})]$ $T_{cell} = c_1 + c_2T_a + c_3G_{tot}+c_4W$	η_{cell}: [148] T_{cell}: [128]
[51]	$\eta_{cell}=\eta_{ref}[1-\beta(T_{cell}-T_{ref})+\gamma\, log_{10}G_{tot}]$ $T_{cell} = T_a + (T_{NOCT}-20)\left(\frac{G_{tot}}{800}\right)$	η_{cell}: [149] and [150] T_{cell}: [151]
[50]	$\eta_{cell}=\eta_{ref}[1-\beta(T_{cell}-T_{ref})+\gamma\, log_{10}G_{tot}]$ $T_{cell} = T_a + c_3G_{tot}$	η_{cell}: [149] and [150] T_{cell}: [130]
[48]	$\eta_{cell}= constant$	η_{cell}: [152] T_{cell}: -
[45]	Detailed in Huld *et al.* (2010)	[131]

*Primary reference is the study that developed and/or first used the equation. It is not necessarily the study that was cited by the authors of the studies, in column 2, to justify the use to estimate P_{pv}. Example: 'A' cites 'B', which cites 'C', which cites 'D'; the primary reference for the study of 'A' is 'D', not 'B'.

** There may be more than one primary reference when the precursor study is not evident.

3.10 Patterns in the impacts of climate change on PV production

Both the qualitative and the quantitative impacts did not show a single trend of results in all the papers analyzed here. A summary of the estimated impacts on PV production due to climate change is presented in Table 8.

3.10.1 Entire globe

The ICC-P_{pv} based on GCMs [43,46] indicated small but generally positive impacts on P_{pv} over the European continent, either in scenario A1B SRES [79] or under RCP8.5 [80]. The decrease in aerosol emissions anticipated in the coming years leads to an escalation in global warming, resulting in notable changes in surface solar radiation and the subsequent productivity of PV energy [45]. Eastern Europe and North Africa exhibit a statistically significant reduction in PV production, with a decline of up to 7%. Conversely, Western Europe and the Eastern

Mediterranean experience a significant increase of up to 10% in PV production.

The utilization of the HadGEM2-CCS model in simulations under the RCP4.5 scenario, specifically employing the Stratospheric Sulfate Injection (SSI) geoengineering method, revealed a decrease in solar energy yield compared to historical levels during the 2040-2059 period. Consequently, a reduction in P_{pv} was observed in Europe, the eastern United States, and eastern Asia, with the exception of Germany [50]. It is worth noting that Germany, being a region with relatively lower insolation, exhibited different outcomes compared to the other regions analyzed.

The contribution to P_{pv} exhibits significant variation depending on the location, with temperature playing a non-negligible role [43]. Following this line, Bazyomo *et al.* (2016) [49] explained that, unlike the research conducted by Wild et al. (2015) [46], the variation in PV production with significant trends does not resemble radiation patterns across the sky. This observation is anticipated, as the air temperature, being the second meteorological variable influencing changes in PV production, exhibits higher values in Western Africa [49]. A similarity shared by both Bazyomo *et al.* (2016) [49] and Wild *et al.* (2015) [46] studies is the negative correlation between P_{pv} and increasing temperature. Consequently, both models project a negative P_{pv} trend for Western Africa. Considering the importance of the trend, the models of Bazyomo *et al.* (2016) [49] that showed positive trend have maximum areas of non-statistical significance. Bazyomo *et al.* (2016) [49] acknowledged that the magnitudes of the trends (whether indicating an increase or reduction in P_{pv}) were relatively small. However, they argued that these trends could potentially increase when considering other factors that were not accounted for in their study, but still influence P_{pv}.

A notable rise in P_{pv} has been observed in Eastern Asia, Europe, Central Africa, and Central America [51]. The decrease in aerosol levels appears to be the primary factor contributing to the increased P_{pv} in Eastern Asia, while significant reductions in aerosols may explain the rise in P_{pv} observed in Europe, Central Africa, and Central America. Conversely, a significant decrease in P_{pv} has been noted in Northern Africa, the Middle East, Central Asia, and Australia, which can be attributed to an increase in aerosols and cloud cover [51].

According to Zhao *et al.* (2020) [5], the most substantial increase in P_{pv} is projected to occur at Guiyang station in China under the RCP8.5 scenario, reaching a value of 31.05% by the end of the 21st century. Specifically, the southern regions of China exhibit a stronger increasing trend in PV energy potential compared to the northern regions. For instance, under RCP8.5, at Guangzhou station, the P_{pv} demonstrates a significant annual increase trend of 0.228% for MPI-ESM-LR compared to trend of 0.105% per year at Hetian station. Furthermore, the results indicate that the increasing trends in P_{pv} under the RCP8.5 scenario are higher than those observed under RCP4.5.

There are discrepancies in the predictions for P_{pv} in China between Crook *et al.* (2011) [43] and Zhao *et al.* (2020) [5]. These differences can be attributed to several factors. Firstly, Zhao *et al.* (2020) [5] utilized high-resolution spatial climate data obtained through statistical downscaling, which may have contributed to more accurate predictions. Additionally, the divergence in predictions can be attributed to Zhao *et al.* (2020) [5] considering the potential increase in P_{pv} due to advancements in PV technology. This consideration was not explicitly accounted for in the earlier work by Crook *et al.* (2011) [43].

The changes in P_{pv} for both winter and summer seasons are anticipated to follow a similar pattern, but the magnitude of these changes varies across different regions [16]. However, in high latitude regions of the Northern Hemisphere, it is expected that the decrease in P_{pv} will be more pronounced during winter compared to summer. This is attributed to the projected substantial increase in cloudiness during the winter season [16,47]. This cloud fraction over the regions of high latitude land is predicted by CMIP5 models project, especially in the regions of and during greatest loss of Arctic Sea Ice [132].

3.10.2 European continent

Based on projections for the end of the 21st century, the variation in PV supply compared to current weather conditions is expected to range from -14% to +2% for Europe. The most significant reductions are anticipated in northern European countries, including a substantial decrease of 10-12% in Scandinavian regions [47].

A reduction in the P_{pv} in Eastern Europe and Northern Africa, equal to 7% was found from simulations carried out by the aerosol-climate model ECHAM5-HAM for 2000-2030 [45]. On the other hand, in Western Europe and in the Eastern Mediterranean significant increases of 10% were projected for the P_{pv} [45]. Building upon the findings of Gaetani *et al.* (2014) [45], Wild *et al.* (2015) [46] provided additional insight by suggesting that P_{pv} is projected to decrease across various regions, including Africa, by the middle of the 21st century.

The Canary Islands in Spain experience relatively smaller and more localized changes in total solar irradiation (G_{tot}) during summer compared to winter. Consequently, there is limited potential for mitigating the decline in P_{pv} resulting from air temperature changes. By the end of the 21st century, under a higher concentration of greenhouse gases (RCP8.5), a

loss of over 5% in P_{pv} is projected across most areas of the Canary Islands [6, 47]. It was reported that the change in P_{pv} has no significance over the next century over the BSc [48]. In Greece, it was projected an increasing P_{pv}, except for the region of Attica, with changes varying from 1 to 2% in most of the study region [44].

The future climate scenarios suggest that the temporal stability of energy production is not significantly compromised, with a minor positive trend observed in southern European countries [47]. Consequently, while certain regions in Europe may experience slight reductions in production, the overall impact of climate change on the European PV sector is not expected to pose a significant threat.

3.10.3 African continent

In the XXI century, it is projected that the P_{pv} will diminish in Africa [46,49], except for Sahel and throughout southwestern Africa, where it is expected to increase [52]. For the West Africa, it was predicted a decrease of P_{pv}, which magnitude grows with warming levels until 3.8% [53]. In general, the projected decrease in P_{pv} is primarily attributed to a combination of reduced solar irradiation and increased temperatures [49, 52].

For the majority of Africa, moderate changes in P_{pv} of less than ±3% are anticipated, with slightly greater reductions projected during the summer season [16, 29, 30, 52]. However, it is important to note that the expected P_{pv} changes in the Sahel region are deemed insignificant due to the uncertainties associated with cloud effects [133].

Regarding Europe, minimal changes are projected in the temporal stability of P_{pv} across all seasons, including daily, annual, and decadal time scales [47, 52].

3.11 Limitations

The key determinant of PV energy among various local weather conditions and environmental factors, including extreme T_a, R_h, precipitation, and W, is the intensity of G_{tot} [134]. However, it is worth noting that losses resulting from other components like rain, wind, and humidity are often disregarded in many studies.

Crook *et al.* (2011) [43] highlighted the significance of various climatic variables that have a notable impact on P_{pv}, some of which are often overlooked. They identified and discussed the following factors: 1) Wind: Wind plays a role in influencing P_{pv} by promoting forced convection, which aids in dissipating heat from the PV cell and subsequently reduces cell temperature; 2) Dust: The accumulation of dust on PV panels can lead to a reduction in absorbed radiation, particularly in arid regions. This poses a significant challenge that affects P_{pv} performance; 3) Rain: Rainfall has the beneficial effect of cleaning PV panels by removing accumulated dust and debris, thereby improving the overall efficiency of energy generation. Considering these variables alongside solar irradiation is crucial for a comprehensive understanding of the factors influencing P_{pv}.

Table 8 - Impacts due to climate change on PV production.

Paper	Period	Increase	Neutral	Decrease
[5]	2006-2100	Southeastern China		To the south of Guangxi, east of Xinjiang and Tibet, west of Qinghai, Henan, Hebei, Shanxi, Shaanxi, Ningxia, parts of Inner Mongolia and Northeastern Central China
[6]	2090-2099			Canary Islands (Spain)
[16]	2036-2065	Central Europe, Atacama Desert, Eastern China, Southeastern Asia, Northeastern USA		Arabian Peninsula, Southeastern Australia and Africa, Southwestern USA and Central Asia
[43]	2010-2080	Spain Germany China	Algeria and Australia	Western United States, Saudi Arabia
[44]	2011-2050 2061-2100	Western and southwestern Greece Epirus Peloponnese Thrace	Macedonia, Crete and Aegean Islands	Attica (Greece), Thessaly (Greece) Attica (Greece), Thessaly (Greece)
[45]	2030	Western Europe and Eastern Mediterranean		Eastern Europe and Northern Africa
[46]	2006-2049	Germany Spain Southeastern China		Northwestern China and Northern India
[47]	2070-2099	Portugal and Spain, Italy, Malta, Bulgaria, Cyprus, Greece, Hungary and Romania		Northern Europe, Western Europe, Central Europe, and Northern Europe
[48]	2071-2100	No significance	No significance	No significance
[49]	2006-2100	Liberia and Sierra Leone		Benin, Burkina Faso, Cape Verde, Côte d'Ivoire, Gambia, Ghana, Guinea-Bissau, Guinea-Conakry, Mali, Niger, Nigeria, Senegal and Togo
[50]	2006-2099	Europe, Eastern United States and Eastern Asia		
[51]	2006-2100	Eastern Asia, Europe, Central Africa, Central America		Northern Africa, Middle East, Central Asia and Australia
[52]	2070-2099	Sub-southern Africa		Northern Africa, Sahara, Western Sahel, Eastern Sahel, Guinea Coast, Eastern Africa, Horn of Africa, Southern Africa
[53]	1.5 2.0 3.0 °C*	-	-	Western Africa

The authors also add some other phenomena, such as large hailstones, which, although rare, have the potential to break PV panels (in some locations they occur more frequently).

Wild *et al.* (2015) [46], in addition to the factors mentioned by Crook *et al.* (2011) [43], also mention the presence of snow, which is not yet considered in existing models. Bazyomo *et al.* (2016) [49] added another component: humidity, which is often neglected. Jerez *et al.* (2015b) [47] commented on the lack of consideration of the inclination of PV modules, although they also do not consider it in their study. It was not observed the fact of taking into account the distribution of the solar spectrum and the effect of air mass [135].

An issue that has been observed is that climate models tend to underestimate the variations in total solar irradiation (G_{tot}) when compared to observations [135]. Similar underestimation issues have been observed in other aspects, such as the irradiation balance at the top of the tropical atmosphere [136], precipitation over land surfaces [137], tropical precipitation specifically [138], soil moisture [139], and diurnal temperature variation [140]. It is evident that these discrepancies highlight the need for improvements in the accuracy of climate models to better capture these important climate variables.

Excessive radiation has long been recognized as a persistent issue in climate modeling [141]. However, there are specific areas, particularly mountainous regions like the Alps, where positive biases in radiation increase by more than 40% [142]. When it comes to irradiation variability, climate models generally exhibit average errors on annual and monthly scales that are predominantly negative, typically below 2%, with occasional instances reaching up to 6% [47]. Efforts to address and reduce these biases in radiation representation remain ongoing in climate modeling research.

The deficiency of RCMs in robustly projecting cloud cover and convection - and, as a consequence, the parameters related to solar irradiation - is criticized [143-144]. This deficiency causes a variability among the different RCMs with order of magnitude higher than the rate of increase in the production derived from monocrystalline PV systems in Greece. For Trenberth and Fasullo (2009) [145], the most important sources of uncertainty are also linked to cloud cover.

It is worth noting that Bartók *et al.* (2017) [57] demonstrated discrepancies between the average solar radiation projections obtained from multi-model ensembles of global climate models (GCMs) and regional climate models (RCMs). These differences can be attributed to the distinct representation of cloud cover in large-scale and smaller-scale models, highlighting the significant influence of cloud cover modeling on the outcomes. Cloud cover plays a crucial role in shaping solar radiation patterns, and the accurate modeling of this parameter is essential for reliable solar energy projections.

The representation of uncertainties related to the indirect effects of natural and anthropogenic aerosols, as well as changes in land use, is limited or often overlooked in regional climate models [45]. These factors, such as natural aerosols like dust from the Sahara and anthropogenic aerosols like air pollution, can have a significant influence on the potential for solar energy production [45]. Their direct and indirect impact on incident solar radiation and on cloud cover, respectively, can lead to substantial modulation of solar irradiation. Additionally, the deposition of aerosols on PV arrays can reduce the efficiency of PV cells. Therefore, considering these factors is crucial for a comprehensive assessment of solar energy potential.

While Gunderson *et al.* (2015) [48] indicate minimal or negligible effects of climate change on solar resources, there are still inaccuracies that need further investigation. Nevertheless, it is evident that land-use alterations will play a substantial role in determining appropriate locations for PV production. Furthermore, allocating a small portion of agricultural land for solar energy generation could greatly enhance the potential for solar power. The study underscores that while solar resources are abundant, it is crucial to consider socio-economic factors as important constraints when evaluating the viability and potential of solar energy.

As already discussed, the increase in temperature induced a reduction in P_{pv} in several regions [47, 49, 52], which confirms the importance of reducing the dependence of PV technology on ambient temperature [146]. Improvement that should happen over time, but it is still not considered in current analysis [147]. Only, in an isolated study [5], the improvement rates for the absolute efficiency of PV technology over time were considered.

4. CONCLUSIONS

In recent years, there has been a growing focus on understanding the effects of climate change on photovoltaic production (P_{pv}). Numerous publications have emerged since 2013, and this ongoing study aims to provide a comprehensive overview of the available evidence, highlighting consistent methodologies for projecting impacts.

The methodologies to evaluate the impacts of climate change on P_{pv} focused mainly on the use of empirical equations that establish relationships between meteorological variables, cell temperature and cell efficiency. Different equations were used to estimate P_{pv}; some considered only the influence of incident solar radiation, while others also considered ambient temperature, and/or wind speed and/or relative humidity. It was observed that dust was not considered in any of the studies reported because it is a good practice to assume that its influence can be overcome by maintenance, so this cost should only be

considered into the financial projections of PV solar installations.

The vast majority of the studies adopted a forecast period of until the end of the 21st century, except for three studies that were limited to shorter periods under the justification of equivalence to the lifespan of PV installations.

Analysis of the articles showed that the data obtained for the projections in the studies came from projects such as CMIP3, CMIP5 and CORDEX. In addition, in the context of GHG emission scenarios, RCP8.5 was the most used, followed by RCP4.5.

The findings of this comprehensive review highlight the significant implications of meteorological changes on PV energy systems and the subsequent impact on energy supply. In the Canary Islands, a loss of over 5% in PV production is projected by the end of the 21st century [6] as well as for Mainland Spain [47]. For Europe, minimal changes in the temporal stability of solar potential are projected across all seasons [47, 52]. In Africa, with the exception of certain regions such as the north coast and 10°S, a decline in average annual solar potential is expected throughout the 21st century, particularly in the Horn of Africa [46, 49, 52]. In contrast, several regions in China are expected to witness a rise in PV energy potential by the end of the XXI century [5]. However, the specific percentage value varies depending on the adopted methodology. Crook *et al.* (2011) [43] suggested only a slight increase in China's PV potential, while Zhao *et al.* (2020) [5] argued for a more substantial increase. Zhao *et al.* (2020) [5] attributed this difference to the utilization of high-resolution spatial climate data obtained through statistical downscaling and the consideration of PV technology advancements.

Regarding the number of studies, it was observed that the majority of studies focused mainly on Europe and Asia; little was studied about the ICC-P_{pv} in South America and Central America.

While this review has identified certain patterns regarding the impacts of climate change on P_{pv}, remains areas that require further investigation. Future literature reviews should adopt a systematic approach to examine the results within the broader context of technological, economic, and environmental considerations.

The economic evaluation should take into account dynamic aspects, including social costs, revenue changes, capacity expansion investment costs, and cost-benefit analysis. From a technological perspective, it is crucial to evaluate the impact of meteorological variations on PV systems, including thermal and electrical fatigue, as well as the potential effects of technological advancements in improving efficiency and reducing dependence on meteorological parameters.

To enhance the understanding of climate change impacts on P_{pv}, future research should also explore the interplay between technological, economic, and environmental factors. By incorporating a systematic review methodology, researchers can provide a more comprehensive analysis of the subject matter. This will enable a deeper understanding of the implications and potential solutions for addressing the challenges posed by climate change in the context of photovoltaic power generation.

This review summarizes useful information to policymakers and entrepreneurs in the field of PV technology against climate change, besides providing basis to clarify to researchers in the field about the current state of the art and thus guide future efforts.

5. ACKNOWLEDGMENTS

The present work was carried out with support from the *Conselho Nacional de Desenvolvimento Científico e Tecnológico* (CNPq) (projects 306783/2018-5 and 308753/2021-6), FAPESQ (project 46924.673.29122.09082021) and PROPESQ/UFPB (project PVK13163-2020).

REFERENCES

[1] Peixóto JP, Oort AH. 1992. The Physics of Climate. USA: American Institute of Physics.

[2] IPCC. 2019. Special Report on Climate Change and Land. Geneva, Switzerland.

[3] Da Guarda ELA, Domingos RMA, Jorge SHM, Durante LC, Sanches JCM, Leão M Callejas IJA. 2020. The influence of climate change on renewable energy systems designed to achieve zero energy buildings in the present: A case study in the Brazilian Savannah. **Sustainable Cities and Society**, v. 52, p. 101843.

[4] IPCC. 2021. Climate Change 2021: The Physical Science Basis. Contribution of Working Group I to the Sixth Assessment Report of the Intergovernmental Panel on Climate Change.

[5] Zhao X, Huang G, Lu C, Zhou X, Li Y. 2020. Impacts of climate change on photovoltaic energy potential: A case study of China. **Applied Energy**, v. 280, 115888.

[6] Pérez JC, González A, Díaz JP, Expósito FJ, Felipe J. 2019. Climate change impact on future photovoltaic resource potential in an orographically complex archipelago, the Canary Islands. **Renewable Energy**, v. 133, 749–759.

[7] Van Ruijven BJ, De Cian E, Sue I. 2019. Wing amplification of future energy demand growth due to climate change. **Nature Communications**, v. 10, 2762.

[8] Bush MJ. 2020. **Climate change and renewable energy: How to end the climate crisis**. 1. ed. Cham: Springer International Publishing p. 525.

[9] Pachauri RK, Mayer L. 2015. Intergovernmental panel on climate change. Climate change 2014: synthesis report. Geneva, Switzerland: Intergovernmental Panel on Climate Change.

[10] Teske S. 2019. **Achieving the Paris Climate Agreement Goals: Global and Regional 100% Renewable Energy Scenarios with Non-energy GHG Pathways for +1.5 °C and +2° C**. 1. ed. Cham: Springer International Publishing. 491 p.

[11] Yang J, Yang Y, Elia Campana P, He J. 2019. City-level analysis of subsidy-free solar photovoltaic electricity price, profits and grid parity in China. **Nature Energy**, v. 4, 709–17.

[12] Polman A, Knight M, Garnett EC, Ehrler B, Sinke WC. 2016. Photovoltaic materials: Present efficiencies and future challenges. **Science**, v. 352, aad4424, 1-10.

[13] Baurzhan S, Jenkins GP. 2016. Off-grid solar PV: Is it an affordable or appropriate solution for rural electrification in Sub-Saharan African countries? **Renewable. Sustainable Energy Reviews** v. 60, p. 1405-1418.

[14] Feron S, Cordero RR, Labbe F. 2017. Rural electrification efforts based on off-grid photovoltaic systems in the Andean region: comparative assessment of their sustainability. **Sustainability**, v. 9, 1825.

[15] Craig MT, Losada Carreño I, Rossol M, Hodge B-M, Brancucci C. 2019. Effects on power system operations of potential changes in wind and solar generation potential under climate change. **Environmental Research Letters**, v. 14, 034014.

[16] Feron S, Cordero RR, Damiani A, Jackson RB. 2021. Climate change extremes and photovoltaic power output. **Nature Sustainability**, v. 4, 270-276.

[17] Ciscar JC, Dowling P. 2014. Integrated assessment of climate impacts and adaptation in the energy sector. **Energy Economics**, v. 46, 531-538.

[18] NOAA. National Oceanic and Atmospheric Administration. The First Climate Model. 2017. Available at: http://celebrating200years.noaa.gov/breakthroughs/ climate_model/. Access on: 04/13/2021.

[19] Pašičko R, Branković C, Šimić Z. 2012. Assessment of climate change impacts on energy generation from renewable sources in Croatia. **Renewable Energy**, v. 46, p. 224–231.

[20] Queiroz AR, Lima LMM, Lima JWM, Silva BC, Scianni LA. 2016. Climate change impacts in the energy supply of the Brazilian hydro-dominant power system. **Renewable Energy**, v. 99, p. 379–389.

[21] Wachsmuth J, Blohm A, Reisemann SG, Eickemeier T, Ruth M, Gasper R, Stührmann, S. 2013. How will renewable power generation be affected by climate change? The case of a Metropolitan Region in Northwest Germany. **Energy**, v. 58, 192–201.

[22] Burnett D, Barbour E, Harrison GP. 2014. The UK solar energy resource and the impact of climate change. **Renewable Energy**, v. 71, 333–343.

[23] Ohunakin OS, Adaramola MS, Oyewola OM, Matthew OJ, Fagbenle RO. 2015. The effect of climate change on solar radiation in Nigeria. **Solar Energy**, v. 116, 272–286.

[24] Huber I, Bugliaro L, Ponater M, Garny H, Emde C, Mayer B. 2016. Do climate models project changes in solar resources? **Solar Energy**, v. 129, 65-84.

[25] Fant C, Adam Schlosser C, Strzepek K. 2016. The impact of climate change on wind and solar resources in southern Africa. **Applied Energy**, v. 161: 556–564.

[26] Gil V, Gaertner MA, Gutierrez C, Losada T. 2018. Impact of climate change on solar irradiation and variability over the Iberian Peninsula using regional climate models. **International Journal Climatology**, joc.5916.

[27] De Jong P, Barreto TB, Tanajura CAS, Kouloukoui D, Oliveira-Esquerre KP, Kiperstok A, *et al.* 2019. Estimating the impact of climate change on wind and solar energy in Brazil using a South American regional climate model. **Renewable Energy**, v. 141, 390–401.

[28] Lawin AE, Niyongendako M, Manirakiza C. 2019. Solar irradiance and temperature variability and projected trends analysis in Burundi. **Climate**, v. 7, 83.

[29] Soares PM, Brito MC, Careto JA. 2019. Persistence of the high solar potential in Africa in a changing climate. **Environmental Research Letters**, v. 14, 124036.

[30] Tang C, Morel B, Wild M, Pohl B, Abiodun B, Bessafi M. 2019a. Numerical simulation of surface solar radiation over southern Africa. Part 1: evaluation of regional and global climate models. **Climate Dynamics**, v. 52, 457–477.

[31] Tang C, Morel B, Wild M, Pohl B, Abiodun B, Lennard C, Bessafi M. 2019b. Numerical simulation of surface solar radiation over southern Africa. Part 2: projections of regional and global climate models. **Climate Dynamics**, v. 53, 2197–2227.

[32] Antonanzas J, Osorio N, Escobar R, Urraca R, Martinez-de-Pison F, Antonanzas-Torres F. 2016. Review of photovoltaic power forecasting. **Solar Energy**, v. 136, 78-111.

[33] Gandoman FH, Raeisi F, Ahmadi A. 2016. A literature review on estimating of PV-array hourly power under cloudy weather

conditions. **Renewable and Sustainable Energy Reviews**, v. 63, 579-592.

[34] Wan C, Zhao J, Song Y, Xu Z, Lin J, Hu Z. 2015. Photovoltaic and solar power forecasting for smart grid energy management. **CSEE J Power Energy Systems** v. 1, 38–46.

[35] Raza MQ, Nadarajah M, Ekanayake C. 2016. On recent advances in PV output power forecast. **Solar Energy**, v. 136, 125–144.

[36] Das UK, Tey KS, Seyedmahmoudian M, Mekhiler S, Idris MYI, Deventer WV, Horan B, Stojcevski A. 2018. Forecasting of photovoltaic power generation and model optimization: A review. **Renewable and Sustainable Energy Reviews**, v. 81, 912-928.

[37] Sobri S, Koohi-Kamali S, Rahim NA. Solar photovoltaic generation forecasting methods: a review. 2018. **Energy Conversion and Management**, v. 156, 459–497.

[38] Akhter MN, Mekhilef S, Mokhlis H, Shah NM. 2019. Review on forecasting of photovoltaic power generation based on machine learning and metaheuristic techniques. **IET Renewable Power Generation**, v. 13 (7), 1009-1023.

[39] Ham-Baloyi WT, Jordan P. 2016. Systematic review as a research method in post-graduate nursing education. **Health SA Gesondheid**, v. 21, p. 120-128.

[40] Emodi NV, Chaiechi T, Beg ABMRA. 2019. The impact of climate variability and change on the energy system: A systematic scoping review. **Science of the Total Environmental**, v. 676, p. 545–563.

[41] Moreno-Guerrero AJ, Gómez-García G, López-Belmonte J, Rodríguez-Jiménez C. 2020. Internet addiction in the Web of Science database: a review of the literature with scientific mapping. **International Journal of Environmental Research and Public Health**, v. 17(8), 1–16.

[42] MICROSOFT. **Excel. 2013**. Available at: https://www.microsoft.com/. Access on: Jul. 13, 2021.

[43] Crook JA, Jones LA, Forster PM, Crook R. 2011. Climate change impacts on future photovoltaic and concentrated solar power energy output. **Energy Environmental Science**, v. 4, 3101-3109.

[44] Panagea IS, Tsanis IK, Koutroulis AG, Grillakis MG. 2014. Climate change impact on photovoltaic energy output: The case of Greece. **Advances in Meteorology,** v. 2014, 264506.

[45] Gaetani M, Huld T, Vignati E, Monforti-Ferrario F, Dosio A, Raes F. 2014. The near future availability of photovoltaic energy in Europe and Africa in climate-aerosol modelling experiments. **Renewable and Sustainable Energy Reviews**, v. 38, 706–716.

[46] Wild M, Folini D, Henschel F, Fischer N, Müller B. 2015. Projections of long-term changes in solar radiation based on CMIP5 climate models and their influence on energy yields of photovoltaic systems. **Solar Energy**, v. 116, 12–24.

[47] Jerez S, Tobin I, Vautard R, Montavez JP, Lopez-Romero JM, Thais F, Bartok B, Christensen OB, Colette A, Deque M, Nikulin G, Kotlarski S, Van Meijgaard E, Teichmann C, Wild M. 2015a. The impact of climate change on photovoltaic power generation in Europe. **Nature Communication**, v. 6, 10014.

[48] Gunderson I, Goyette F, Gago-Silva A, Quiquerez L, Lehmann A. 2015. Climate and land-use change impacts on potential solar photovoltaic power generation in the Black Sea region, **Environmental Science e Policy**, v. 46, 70-81.

[49] Bazyomo SDYB, Lawin EA, Coulibaly O, Ouedraogo A. 2016. Forecasted Changes in West Africa Photovoltaic Energy Output by 2045. **Climate**, v. 4, 53.

[50] Smith CJ, Crook JA, Crook R, Jackson LS, Osprey SM, Forster PM. 2017. Impacts of Stratospheric Sulfate Geoengineering on Global Solar Photovoltaic and Concentrating Solar Power Resource. **Journal of Applied Meteorology and Climatology**, v. 56, 1483-1497.

[51] Zou L, Wang L, Li J, Lu Y, Gong W, Niu Y. 2019. Global surface solar radiation and photovoltaic power from coupled model intercomparison project phase 5 climate models. **Journal of Cleaner Production**, v. 224, 304–324.

[52] Bichet A, Hingray B, Evin G, Diedhiou A, Kebe CMF, Anquetin S. 2019. Potential impact of climate change on solar resource in Africa for photovoltaic energy: analyses from CORDEX-AFRICA climate experiments. **Environmental Research Letters**, v. 14, 124039.

[53] Sawadogo W, Abiodun BJ, Okogbue EC. 2020. Impacts of global warming on photovoltaic power generation over West Africa. **Renewable Energy**, v. 151, 263-277.

[54] Diagne M, David M, Lauret P, Boland J, Schmutz N. 2013. Review of solar irradiance forecasting methods and a proposition for small-scale insular grids. **Renewable and Sustainable Energy Reviews,** v. 27, 65–76.

[55] Macguffie K, Henderson-Sellers A. 2006. **A Climate Modelling Primer**. 3. ed. John Wiley and Sons: Chichester, 288 p.

[56] Torma CS, Giorgi F, Coppola E. 2015. Added value of regional climate modeling over areas characterized by complex terrain—precipitation over the Alps. **Journal of**

Geophysical Research: Atmospheres, v. 120, 3957–3972.

[57] Bartók B, Wild M, Folini D, Lüthi D, Kotlarski S, Schär C, Vautard R, Jerez S, Imecs Z. 2017. Projected changes in surface solar radiation in CMIP5 global climate models and in EURO-CORDEX regional climate models for Europe. **Climate Dynamics,** v. 49, 2665–2683.

[58] Christensen JH, Carter TR, Rummukainen M, Amanatidis G. 2007. Evaluating the performance and utility of regional climate models: the PRUDENCE project. **Climate Change**, v. 81, 1–6.

[59] Chen C, Duan S, Cai T, Liu B. 2011. Online 24-h solar power forecasting based on weather type classification using artificial neural network. **Solar Energy**, v. 85, 2856–2870.

[60] CMIP5. 2013. Coupled Model Intercomparison Project Phase 5. http://cmip-pcmdi.llnl.gov/cmip5. Last accessed on 5 November 2020.

[61] Wild M, Long CN, Ohmura A. 2006. Evaluation of clear-sky solar fluxes in GCMs participating in AMIP and IPCC-AR4 from a surface perspective. **Journal of Geophysical Research**, v. 111, D01104.

[62] Huang G. 1992. A stepwise cluster analysis method for predicting air quality in an urban environment. **Atmospheric Environment. Part B. Urban Atmosphere**, v. 26, 349–357.

[63] Wilks SS. 1932. Certain generalizations in the analysis of variance. **Biometrika**, v. 24, 471–94.

[64] Jerez S, Thais F, Tobin I, Wild M, Colette A, Yiou P, Vautard R. 2015b. The CLIMIX model: A tool to create and evaluate spatially-resolved scenarios of photovoltaic and wind power development. **Renewable and Sustainable Energy Reviews**, v. 42, 1-15.

[65] Lehmann A, Giuliani G, Mancosu E, Abbaspour KC, Sözen S, Gorgan D, Beel A, Ray N. 2015. Filling the gap between earth observation and policy making in the Black Sea catchment with enviroGRIDS. **Environmental Science and Policy**, v. 46, 1–12.

[66] Skamarock WC, Klemp JB, Dudhia J, Gill DO, Barker M, Duda KG, Huang XY, Wang W, Powers JG. 2008. A description of the advanced research WRF Version 3, technical report, National Center for Atmospheric Research.

[67] Kimura F, Kitoh A. 2007. Downscaling by Pseudo Global Warming Method, The Final Report of ICCAP 4346.

[68] Perpiñán O. 2012. solaR: Solar Radiation and photovoltaic Systems with R. **Journal of Statistical Software**, v., 50(9), 1–32.

[69] Van Vuuren DP, Edmonds J, Kainuma M, Riahi K, Thomson A, Hibbard K, Hurtt GC, Kram T, Krey V, Lamarque, J-F, *et al.* 2011. The representative concentration pathways: an overview. **Climatic Change**, v. 109 (1–2), 5–31.

[70] Thomson AM, Calvin KV, Smith SJ, Kyle GP, Volke A, Patel P, *et al.* 2011. RCP4.5: a pathway for stabilization of radiative forcing by 2100. **Climatic Change**, v. 109, 177.

[71] Riahi K, Rao S, Krey V, Cho C, Chirkov V, Fischer G, *et al.* 2011. RCP 8.5-A scenario of comparatively high greenhouse gas emissions. **Climatic Change**, v. 109 (1–2), 33–57.

[72] Sato T, Kimura F, Kitoh A. 2007. Projection of global warming onto regional precipitation over Mongolia using a regional climate model. **Journal of Hydrology**, v. 333 (1), 144-154.

[73] Kawase H, Yoshikane T, Hara M, Kimura F, Yasunari T, Ailikun B, Ueda H, Inoue T. 2009. Intermodel variability of future changes in the Baiu rainband estimated by the pseudo global warming downscaling method. **Journal of Geophysical. Research**, v. 114.

[74] Kawase H, Yoshikane T, Hara M, Ailikun B, Kimura F, Yasunari T. 2008. Downscaling of the climatic change in the Mei-yu rainband in East Asia by a pseudo climate simulation method. **SOLA**, v. 4, 73-76.

[75] Lauer A, Zhang C, Elison-Timm O, Wang Y, Hamilton K. 2013. Downscaling of climate change in the Hawaii region using CMIP5 results: on the choice of the forcing fields. **Journal of Climate**, v. 26 (24), 10006-10030.

[76] WMO. 2011. Guide to Climatological Practices/World Meteorological Organization, 2011th Edition, World Meteorological Organization, Geneva, Switzerland. http://www.wmo.int/pages/prog/wcp/ccl/guide/documents/WMO_100_en.pdf.

[77] Déqué M, Calmanti S, Christensen OB, Aquila Dell A, Maule CF, Haensler A, Nikulin G, Teichmann C. 2017. A multi-model climate response over tropical Africa at +2 °C. **Climate Services**, v. 7, 87-95.

[78] Taylor KE, Stouffer RJ, Meehl GA. 2012. An overview of CMIP5 and the experiment design. **Bulletin of the American Meteorological Society**, v. 93 (4), 485–498.

[79] IPCC. 2013. Special Report on Emissions Scenarios. Cambridge Univ. Press.

[80] Moss RH, Edmonds JA, Hibbard KA, Manning MR, Rose SK, Van Vuuren DP, Carter TR, Emori S, Kainuma M, Kram T, *et al.* 2010. The next generation of scenarios for climate change research and assessment. **Nature**, v. 463 (7282), 747–756.

[81] Eyring V, Bony S, Meehl GA, Senior CA, Stevens B, Stouffer RJ, Taylor KE. 2016. Overview of the Coupled Model Intercomparison Project Phase 6 (CMIP6) experimental design and organization.

Geoscientific Model Development, v. 9, 1937-1958.

[82] Jacob D, Petersen J, Eggert B, Alias A, Christensen OB, Bouwer LM, *et al.* 2014. EURO-CORDEX: new high-resolution climate change projections for European impact research. **Regional Environmental Change**, v. 14, 563–578.

[83] CORDEX. 2021. Coordinated Regional Climate Downscaling Experiment. https://cordex.org/. Last accessed on 22 March 2021.

[84] Nikulin G, Jones C, Giorgi F, Asrar G, Büchner M, Cerezo-Mota R, *et al.*, 2012. Precipitation climatology in an ensemble of CORDEX-Africa regional climate simulations. **Journal of Climate**, v. 25 (18), 6057-6078.

[85] Martínez-Durbán M, Zarzalejo LF, Bosch JL, Rosiek S, Polo J, Batlles FJ. 2009. Estimation of global daily irradiation in complex topography zones using digital elevation models and meteosat images: comparison of the results. **Energy Conversion and Management**, v. 50, 2233–2238.

[86] Aguilar C, Herrero J, POLO MJ. 2010. Topographic effects on solar radiation distribution in mountainous watersheds and their influence on reference evapotranspiration estimates at watershed scale. **Hydrology and Earth System Sciences**, v. 7, 2373–2411.

[87] Ruiz-Ariás JA, Pozo-Vázquez D, Santos-Alamillos FJ, Lara-Fanego V, Tovar-Pescador J. 2011. A topographic geostatistical approach for mapping monthly mean values of daily global solar radiation: a case study in southern Spain. **Agricultural and Forest Meteorology**, v. 151, 1812–1822.

[88] Alsamamra H, Ruiz-Arias JA, Pozo-Vázquez D, Tovar-Pescador J. 2009. A comparative study of ordinary and residual kriging techniques for mapping global solar radiation over southern Spain. **Agricultural and Forest Meteorology**, v. 149, 1343–1357.

[89] Tovar-Pescador J, Pozo-Vázquez D, Ruiz-Ariás JA, Batlles J, López G, Bosch JL. 2006. On the use of the digital elevation model to estimate the solar radiation in areas of complex topography. **Meteorology Applied**, v. 13, 279–287.

[90] Arán-Carrión J, Espín Estrella A, Aznar Dols F, Ramos Ridao A. 2008. The electricity production capacity of photovoltaic power plants and the selection of solar energy sites in Andalusia (Spain). **Renewable Energy**, v. 33, 545–552.

[91] Lobell DB, Bonfils C, Duffy PB. 2007. Climate change uncertainty for daily minimum and maximum temperatures: A model inter-comparison. **Geophysical Research Letters**, v. 34 (5), L05715.

[92] Suehrcke H. 2000. On the relationship between duration of sunshine and solar radiation on the Earth's surface: Ångstrom's equation revisited. **Solar Energy**, v. 68 (5), 417-425.

[93] Wild M. 2008. Short-wave and long-wave surface radiation budgets in GCMs: a review based on the IPCC-AR4/CMIP3 models. **Tellus A: Dynamic Meteorology and Oceanography**, v. 60 (5), 932–945.

[94] Mueller B, Seneviratne SI. 2014. Systematic land climate and evapotranspiration biases in CMIP5 simulations. **Geophysical Research Letters**, v. 41.

[95] Stanfield RE, Dong X, Xi B, Kennedy A, Genio ADD, Minnis P, *et al.* 2014. Assessment of NASA GISS CMIP5 and post-CMIP5 simulated clouds and TOA radiation budgets using satellite observations. Part I: Cloud fraction and properties. **Journal of Climate**, v. 27 (11), 4189–4208.

[96] Haerter JO, Hagemann S, Moseley C, Piani, C. 2011. Climate model bias correction and the role of timescales. **Hydrology and Earth System Sciences**, v. 15 (3), 1065–1079.

[97] Christensen JH; Boberg F, Christensen OB; Lucas-Picher P. 2008. On the need for bias correction of regional climate change projections of temperature and precipitation. **Geophysical Research Letters**, v. 35 (20), L20709.

[98] Terink W, Hurkmans RTWL; Torfs PJJF, Uijlenhoet R. 2009. Bias correction of temperature and precipitation data for regional climate model application to the Rhine basin. **Hydrology and Earth System Sciences Discussions**, v. 6 (4), 5377–5413.

[99] Boberg F, Christensen JH. 2012. Overestimation of Mediterranean summer temperature projections due to model deficiencies. **Nature Climate Change**, v. 2 (6), 433–436.

[100] Müller B, Wild M, Driesse A, Behrens K. 2014. Rethinking solar resource assessments in the context of global dimming and brightening. **Solar Energy**, v. 99, 272–282.

[101] Dee DP, Uppala SM, Simmons AJ, Berrisford P, Poli P, Kobayashi S, *et al.* 2011. The ERA-Interim reanalysis: configuration and performance of the data assimilation system. **Quarterly Journal of the Royal M Meteorological Society**, v. 137, 553–597.

[102] MPIMET, 2020. Climate Data Operators. Available online: http://www.mpimet.mpg.de/cdo Access on: 07/01/2020.

[103] R Development Core R. R: A Language and Environment for Statistical Computing; R Foundation for Statistical Computing: Vienna, Austria, 2008.

[104] Expósito FJ, González A, Pérez JC, Díaz JP, Taima D. 2015. High-resolution future

projections of temperature and precipitation in the canary islands. **Journal of Climate**, v. 28 (19), 7846-7856.

[105] González A, Pérez JC, Díaz JP, Expósito FJ. 2017. Future projections of wind resource in a mountainous archipelago, Canary Islands. **Renewable Energy**, v. 104, 120-128.

[106] Wilks D. 1997. Resampling hypothesis tests for autocorrelated fields. **Journal of Climate**, v. 10 (1), 65-82.

[107] Wallach D, Mearns LO, Ruane AC, Rötter RP, Asseng S. 2016. Lessons from climate modeling on the design and use of ensembles for crop modeling, **Climatic Change**, v. 139 (3-4), 551-564.

[108] Hagedorn R, Doblas-Reyes FJ, PALMER TN. 2005. The rationale behind the success of multi-model ensembles in seasonal forecasting – I. Basic concept. **Tellus A: Dynamic Meteorology and Oceanography**, v. 57 (3), 219-233.

[109] Al Samouly A, Luong CN, Li Z, Smith S, Baetz B, Ghaith M. 2018. Performance of multi-model ensembles for the simulation of temperature variability over Ontario, Canada. **Environmental Earth Sciences**, v. 77 (13), 524.

[110] Houghton JT, Ding Y, Griggs DJ, Noguer M, Van Der Linden PJ, DAI X, *et al.* 2001. Contribution of working group I to the third assessment report of the intergovernmental panel on climate change. Clim. Change 2001: The Scientific Basis.

[111] Evin G, Hingray B, Blanchet J, Eckert N, Morin S, Verfaillie D. 2019. Partitioning uncertainty components of an incomplete ensemble of climate projections using data augmentation. **Journal of Climate**, v. 32, 2423–2440.

[112] Hingray B, Saïd M. 2014. Partitioning internal variability and model uncertainty components in a multimember multimodel ensemble of climate projections. **Journal of Climate**, v. 27 6779–6798.

[113] Gutiérrez C, Somot S, Nabat P, Mallet M, Corre L, Van Meijgaard E, Perpiñán O, Gaertner. 2020. Future evolution of surface solar radiation and photovoltaic potential in Europe: investigating the role of aerosols. **Environmental Research Letters**, v. 15, 034035.

[114] Lelieveld J, Berresheim H, Borrmann S, Crutzen PJ, Dentener FJ, Fischer H. *et al.* 2002. Global air pollution crossroads over the Mediterranean. **Science**, v. 298, 794–799.

[115] Li X, Mauzerall DL, Bergin MH. 2020. Global reduction of solar power generation efficiency due to aerosols and panel soiling. **Nature Sustainable**, v.3, 720–727.

[116] Chen SA, Vishwanath A, Sathe S, Kalyanaraman S. 2016. Shedding light on the performance of solar panels: a data-driven view. **SIGKDD Explorations Newsletter**, v. 17, 24–36.

[117] Chaichan MT, Kazem HA. 2016. Experimental analysis of solar intensity on photovoltaic in hot and humid weather conditions. **International Journal Scientific e Engineering Research**, v. 7, 91–96.

[118] Chenni R, Makhlouf M, Kerbache T, Bouzid A. 2007. A detailed modeling method for photovoltaic cells. **Energy**, v. 32, 1724–1730.

[119] Evans DL. 1981. Simplified method for predicting photovoltaic array output. **Solar Energy**, v. 27, 555–560.

[120] Zondag HA. 2008. Flat-plate PV-Thermal collectors and systems: A review. **Renewable Sustainable Energy Reviews**, v. 12, 891–959.

[121] Skoplaki E, Palyvos JA. 2009. On the temperature dependence of photovoltaic module electrical performance: a review of efficiency/power correlations. **Solar Energy**, v. 83, 614–624.

[122] Lasnier F, Ang TG. 1990. **Photovoltaic Engineering Handbook**. 1. ed. Adam Hilger: Nova Iorque. 572 p.

[123] Kou Q, Klein SA, Beckman WA. 1998. A method for estimating the long-term performance of direct-coupled PV pumping systems. **Solar Energy**, v. 64 (1-3), 33–40.

[124] Duffie JA, Beckman WA. 2006. **Solar Energy Thermal Processes**. 3 ed., Wiley, Hoboken, NJ.

[125] Omar AM, Shaari S, Hussin MZ, Sopian KB. 2014. Energy yield calculation of the grid connected photovoltaic power system. **Computer Applications in Environmental Sciences and Renewable Energy**, 162-167.

[126] Tonui JK, Tripanagnostopoulos Y. 2008. Performance improvement of PV/T solar collectors with natural air flow operation. **Solar Energy**, v. 82, 1–12.

[127] Mavromatakis F, Kavoussanaki, E, Vignola F, Franghiadakis, Y. 2014. Measuring and estimating the temperature of photovoltaic modules. **Solar Energy**, v. 110, 656-666.

[128] Tamizhmani G, Ji L, Tang Y, Petacci L, Osterwald C. 2003. Photovoltaic module thermal/wind performance: long-term monitoring and model development for energy rating, in: **NCPV and Solar Program Review Meeting**, v. 1, 936-939.

[129] Mekhilef S, Saidur R, Kamalisarvestani M. 2012. Effect of dust, humidity and air velocity on efficiency of photovoltaic cells. **Renewable and Sustainable Energy Reviews,** v. 16 (5), 2920-2925.

[130] Skoplaki E, Boudouvis AG, Palyvos JA. 2008. A simple correlation for the operating temperature of photovoltaic modules of arbitrary mounting. **Solar Energy Materials and Solar Cells**, v. 92, 1393–1402.

[131] Huld T, Gottschalg R, Beyer HG, Topic M. 2010. Mapping the performance of PV modules, effects of module type and data averaging. **Solar Energy**, v. 84, 324–338.

[132] Vihma T, Screen J, Tjernström M, Newton B, Zhang X, Popova V, *et al.* 2016. The atmospheric role in the Arctic water cycle: a review on processes, past and future changes, and their impacts. **Journal Geophysical Research: Biogeosciences**. v. 121, 586–620.

[133] Biasutti M. 2013. Forced Sahel rainfall trends in the CMIP5 archive. **Journal of Geophysical Research: Atmospheres**, v. 118, 1613–1623.

[134] Bhattacharjee S, Bhakta S. 2013. Analysis of system performance indices of PV generator in a cloudburst precinct. **Sustainable Energy Technologies Assessment**, v. 4, 62–71.

[135] De Soto W, Klein SA, Beckman WA. 2006. Improvement and validation of a model for photovoltaic array performance. **Solar Energy**, v. 80, 78–88.

[136] Allen RJ, Norris JR, Wild M. 2013. Evaluation of multidecadal variability in CMIP5 surface solar radiation and inferred underestimation of aerosol direct effects over Europe, China, Japan, and India. **Journal of Geophysical Research: – Atmospheres**, v. 118 (12), 6311–6336.

[137] Wielicki BA, Wong T, Allan RP, Slingo A, Kiehl JT, Soden BJ, *et al.* 2002. Evidence for large decadal variability in the tropical mean radiative energy budget. **Science**, v. 295 (5556), 841–844.

[138] Wild M, Liepert B. 2010. The earth radiation balance as driver of the global hydrological cycle. **Environmental Research Letters**, v. 5 (2), 025003.

[139] Allan RP, Soden BJ. 2007. Large discrepancy between observed and simulated precipitation trends in the ascending and descending branches of the tropical circulation. **Geophysical Research Letter.**, v. 34 (18), L18705.

[140] Li HB, Robock A, Wild M. 2007. Evaluation of intergovernmental panel on climate change fourth assessment soil moisture simulations for the second half of the twentieth century. **Journal of Geophysical Research: Atmospheres**, v. 112, D06106.

[141] Wild M. 2009a How well do IPCC-AR4/CMIP3 climate models simulate global dimming/brightening and twentieth-century daytime and nighttime warming? **Journal of Geophysical Research Atmospheres**, v. 114, D00d11.

[142] Wild M. *et al.* 2013. The global energy balance from a surface perspective**. Climate Dynamics**, v. 40, 3107–3134.

[143] Hakuba MZ, Folini D, Sanchez-Lorenzo A, Wild M. 2013. Spatial representativeness of ground-based solar radiation measurements. **Journal of Geophysical Research: Atmospheres**, v. 118, 8585–8597.

[144] Lara-Fanego V, Ruiz-Arias JA, Pozo-Vázquez D, Santos-Alamillos FJ, Tovar-Pescador J. 2012. Evaluation of the WRF model solar irradiance forecasts in Andalusia (southern Spain). **Solar Energy**, v. 86, 2200–2217.

[145] Trenberth KE, Fasullo JT. 2009. Global warming due to increasing absorbed solar radiation. **Geophysical Research Letters**, v. 36, L07706.

[146] Patt A, Pfenninger S, Lilliestam J. 2013. Vulnerability of solar energy infrastructure and output to climate change. **Climate Change**., v. 121, 93–102.

[147] Müller J, Folini D, Wild M, Pfenninger S. 2019. CMIP-5 models project photovoltaics are a no-regrets investment in Europe irrespective of climate change. **Energy**, v. 171, 135-148.

[148] Lewis CA, Kirkpatric JP. Solar cell characteristics at high solar intensities and temperatures. 8th IEEE Photovoltaic Specialists Conf. Record, 123-134. Seattle, Washington, 1970.

[149] Evans DL, Florschuetz LW. Cost studies on terrestrial photovoltaic power systems with sunlight concentration. **Solar Energy**, v. 19,255–262, 1977.

[150] Spectrolab. Photovoltaic systems concept study. Rep. AL0-2748-12, Inc., Sylmar, CA, 1977.

[151] Ross RG, Smokler MI. Report: Electricity from Photovoltaic Solar Cells: Flat-Plate Solar Array. Project Final Report. California. 1986.

[152] Sorensen B. 2001. GIS management of solar resource data. **Solar Energy Materials and Solar Cells**, v. 67, 503–509.